



The *in vitro* effects of Cannabidiol on high glucose levels with miRNA profiling

by

Chanelle Rinkwest

(212270346)

Research

Thesis submitted in fulfilment of the requirements for the degree

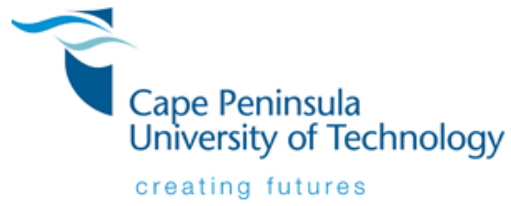
Master of Science (MSc): Biomedical Technology

In the Faculty of Health and Wellness Sciences, Department of Biomedical Sciences

At the Cape Peninsula University of Technology

Supervisor: Dr S Raghubeer

Co-Supervisor: Prof T.E Matsha



CPUT copyright information

The dissertation/thesis may not be published either in part (in scholarly, scientific, or technical journals), or as a whole (as a monograph), unless permission has been obtained from the University.

DECLARATION

I, Chanelle Nicole Rinkwest, declare that the contents of this dissertation/thesis represent my own unaided work, and that the dissertation/thesis has not previously been submitted for academic examination towards any qualification. Furthermore, it represents my own opinions and not necessarily those of the Cape Peninsula University of Technology.

Signed: 

Date: 18/11/2024

ABSTRACT

Background: Diabetes is a group of metabolic disorders caused by defects in insulin action, insulin secretion, or both. Diabetes mellitus (DM) is characterised by a chronic hyperglycaemic state. The International Diabetes Federation (IDF) estimated that 456 million adults presented with diabetes in 2017. It is projected that there will be 693 million cases of diabetes by 2045. Oxidative stress plays a role in the pathogenesis of DM, and further research must be conducted to identify therapeutic initiatives to combat oxidative stress to prevent the onset and progression of DM. One of the most consumed drugs worldwide is Cannabis, which is consumed by an estimated 200-300 million people. Research has shown that cannabis may possess antioxidant properties. Cannabis contains more than 545 known compounds and 86 cannabinoid chemicals. The main psychoactive chemical is tetrahydrocannabinol (THC), other cannabinoid chemicals include cannabidiol (CBD) and cannabinol (CBN). Due to the growing burden on the South African health care system, finding innovative ways to treat or prevent DM will be very helpful. The aim of this study is to investigate the biochemical effects of CBD in high glucose conditions in an *in vitro* liver model.

Methodology: Cells were exposed to high glucose (40 mM), low (1 μ M) CBD concentration and high (5 μ M) CBD concentrations, and a combination of glucose and CBD concentrations for 48 and 72 hours. Quantitative real-time PCR was used to measure oxidative stress genes, including *PPARG*, *SOD*, *NRF2*, *NF- κ B*, *HIF1A*, *GPX*, and *CAT*, as well as miRNA-34a expression. Multiplex assays were used to measure the concentration of inflammatory cytokines, including of IL-6, IL-9, IL-10 and PDGF-BB.

Results: Our results demonstrate significant downregulation of *CAT*, *SOD*, and *Nrf2* genes in response to glucose. At 72 hours, CBD upregulated *SOD* and reversed glucose-induced downregulation of *CAT*, suggesting an opposing effect of CBD on glucose-induced oxidative stress. Additionally, CBD modulated the expression of *PPARG*, *HIF-1 α* , *NF- κ B*, and miRNA-34a, with differential effects depending on exposure duration and concentration. Inflammatory cytokines IL-6, IL-8, and IL-9 exhibited varied responses to glucose and CBD, indicating that CBD may modulate the immune response, with higher doses generally exerting a protective or regulatory effect. PDGF-BB levels were reduced by CBD at 48 hours but increased at 72 hours, suggesting CBD's potential role in cellular repair processes over time.

Conclusion: These findings highlight CBD's capacity to counteract some of the detrimental effects of hyperglycaemia, although further research is needed to optimize dosing and fully elucidate the underlying mechanisms.

ACKNOWLEDGEMENTS

I would like to thank:

My supervisor, Dr Shanel Raghubeer for her guidance and support throughout my MSc thesis

My co-supervisor, Prof Tandi Matsha

Ms Abegail Tshivhase for her assistance in the laboratory

My fellow students for their help and support

My family for all the support and motivation

GES Labs for donating the CBD isolate that was used to perform the experiments.

HWSETA for the bursaries

This research project was supported by grants from the South African Medical Research Council (SAMRC), with funds from National Treasury under its Economic Competitiveness and Support Package (MRC-RFA-UFSP-01-2013/VMH Study), South African National Research Foundation (SANRF) grant no. 115450). Any opinions, findings, conclusions or recommendations expressed in this article are those of the authors, and the SAMRC and/or SANRF do not accept any liability in this regard.

TABLE OF CONTENTS

DECLARATION.....	3
ABSTRACT	4
ACKNOWLEDGEMENTS	5
LIST OF FIGURES	8
LIST OF TABLES.....	10
CHAPTER ONE.....	13
1.1 DIABETES AND INSULIN RESISTANCE	13
1.2 THE ENDOCANNABINOID SYSTEM	14
1.3 THE LIVER.....	16
1.4 OXIDATIVE STRESS PATHWAYS.....	17
1.5 CANNABIS AND CANNABINOID COMPOUNDS.....	20
1.6 THE LAWS REGARDING CBD USE IN SOUTH AFRICA	22
1.7 THE EFFECTS OF CBD.....	22
1.8 MIRNAS.....	23
1.9 STUDY RATIONALE	24
1.10 AIMS AND OBJECTIVES	25
1.10.1 AIM.....	25
1.10.2 OBJECTIVES	25
1.11 HYPOTHESIS	25
CHAPTER TWO.....	26
METHODOLOGY.....	26
2.1 MATERIALS	26
2.2 METHODS.....	26
2.2.1 STUDY DESIGN	26
2.2.2 CELL CULTURE.....	26
2.2.3 RNA ISOLATION	27
2.2.4 RNA QUANTIFICATION AND STANDARDISATION	29
2.2.5 CDNA SYNTHESIS USING THE ISCRIPT CDNA SYNTHESIS KIT	29
2.2.6 REAL TIME PCR FOR GENE EXPRESSION USING BIO-RAD SSOADVANCED UNIVERSAL SYBR GREEN SUPERMIX	29
2.2.7 MICRORNA EXTRACTION	32
2.2.9 REAL-TIME PCR USING THE MIRCURY LNA SYBR GREEN PCR KIT.....	34
2.2.10 BIO-PLEX PRO HUMAN CYTOKINE ASSAY	35

2.2.11 DATA ANALYSIS.....	36
2.12 ETHICAL STATEMENT	36
<u>CHAPTER THREE.....</u>	<u>37</u>
RESULTS	37
3.1 SOD AND CAT GENE EXPRESSION	37
3.2 GPX AND NRF2 GENE EXPRESSION	39
3.3 PPARG AND HIF1A GENE EXPRESSION.....	41
3.4 NF-KB GENE EXPRESSION.....	43
3.5 MIRNA 34A GENE EXPRESSION	44
3.6 IL-6 CYTOKINE CONCENTRATIONS.....	44
3.7 IL-8 CYTOKINE CONCENTRATIONS.....	45
3.8 IL-9 CYTOKINE CONCENTRATIONS.....	46
3.9 PDGF-BB CYTOKINE CONCENTRATIONS	47
<u>CHAPTER FOUR.....</u>	<u>49</u>
DISCUSSION.....	49
<u>CHAPTER FIVE.....</u>	<u>54</u>
LIMITATIONS.....	54
CONCLUSION.....	54
<u>REFERENCES</u>	<u>55</u>
<u>APPENDIX A.....</u>	<u>66</u>

LIST OF FIGURES

Chapter 1

Figure 1.1. The metabolic processing of glucose in the human liver (Adeva-Andany, 2016).

Figure 1.2. Location and distribution of CB1 and CB2 receptors in the human body (Muralidhar, 2019).

Figure 1.3. Redox cycles linking metabolic and antioxidant pathways (Mendez, 2017).

Figure 1.4. Different pathways and genes that are involved in oxidative stress (Liu, 2022).

Figure 1.5. Chemical Structure of CBD (Atalay, 2019).

Figure 1.6. The miRNA formation process involves two maturation stages driven by the RNase enzymes Dicer and Drosha. The initial step occurs within the nucleus, while the subsequent step occurs in the cytoplasm, resulting in the creation of two distinct miRNA strands. The mature guide strand derived from this process can execute either translational repression or mRNA degradation functions (Sand, 2014).

Chapter 2

Figure 2. The extraction method used for RNA isolation (<https://www.addgene.org/protocols/kit-free-rna-extraction/>).

Chapter 3

Figure 3.1. Expression of superoxide dismutase (*SOD*; A and B) and catalase (*CAT*; C and D) in HepG2 cells treated with high glucose (40 mM) and CBD (1 μ M and 5 μ M) over 48 and 72 hours. The mRNA expression was quantified using qPCR. *GAPDH* was used as the housekeeping gene. * $p < 0.05$, ** $p < 0.01$, *** $p < 0.001$, and **** $p < 0.0001$ indicate levels of significance. C, Control; G, glucose; LCBD, low CBD; HCBD, high CBD; LCBD+G, low CBD with glucose; HCBD+G, high CBD with glucose.

Figure 3.2. Expression of glutathione peroxidase (*GPX*; A and B) and nuclear factor erythroid 2-related factor 2 (*NRF2*; C and D) in HepG2 cells treated with high glucose (40 mM) and CBD (1 μ M and 5 μ M) over 48 and 72 hours. The mRNA expression was quantified using qPCR. *GAPDH* was used as the housekeeping gene. * $p < 0.05$, ** $p < 0.01$, *** $p < 0.001$, and **** $p < 0.0001$ indicate levels of significance. C, Control; G, glucose; LCBD, low CBD; HCBD, high CBD; LCBD+G, low CBD with glucose; HCBD+G, high CBD with glucose.

Figure 3.3. Expression of peroxisome proliferator activated receptor gamma (*PPARG*; A and B) and hypoxia-inducible factor 1alpha (*HIF1A*; C and D) in HepG2 cells treated with high glucose (40 mM) and CBD (1 μ M and 5 μ M) over 48 and 72 hours. The mRNA expression was quantified using qPCR. *GAPDH* was used as the housekeeping gene. * $p < 0.05$, ** $p < 0.01$, *** $p < 0.001$, and **** $p < 0.0001$. C, Control; G, glucose; LCBD, low CBD; HCBD, high CBD; LCBD+G, low CBD with glucose; HCBD+G, high CBD with glucose.

Figure 3.4. Expression of nuclear factor kappa-light-chain-enhancer of activated B cells (*NF- κ B*) in HepG2 cells treated with high glucose (40 mM) and CBD (1 μ M and 5 μ M) over 48 hours (A) and 72 hours (B). The mRNA expression was quantified using qPCR. *GAPDH* was used as the housekeeping gene. * $p < 0.05$, ** $p < 0.01$, *** $p < 0.001$, and **** $p < 0.0001$. C, Control; G, glucose; LCBD, low CBD; HCBD, high CBD; LCBD+G, low CBD with glucose; HCBD+G, high CBD with glucose.

Figure 3.5. Expression of miRNA-34a in HepG2 cells treated with high glucose (40 mM) and CBD (1 μ M and 5 μ M) over 48 hours (A) and 72 hours (B). The miRNA expression was quantified using qPCR. U6 SnRNA (V2) was used as the housekeeping gene. * $p < 0.05$, ** $p < 0.01$, *** $p < 0.001$ and **** $p < 0.0001$. C, Control; G, glucose; LCBD, low CBD; HCBD, high CBD; LCBD+G, low CBD with glucose; HCBD+G, high CBD with glucose.

Figure 3.6. Concentrations of HU-IL-6 cytokine in HepG2 cells treated with high glucose (40 mM) and CBD (1 μ M and 5 μ M) over 48 (A) and 72 hours (B). * $p < 0.05$, ** $p < 0.01$, *** $p < 0.001$, and **** $p < 0.0001$. C, Control; G, glucose; LCBD, low CBD; HCBD, high CBD; LCBD+G, low CBD with glucose; HCBD+G, high CBD with glucose.

Figure 3.7. Concentrations of HU-IL-8 cytokine in HepG2 cells treated with high glucose (40 mM) and CBD (1 μ M and 5 μ M) over 48 (A) and 72 hours (B). * $p < 0.05$, ** $p < 0.01$, *** $p < 0.001$, and **** $p < 0.0001$. C, Control; G, glucose; LCBD, low CBD; HCBD, high CBD; LCBD+G, low CBD with glucose; HCBD+G, high CBD with glucose.

Figure 3.8. Concentrations of HU-IL-9 cytokine in HepG2 cells treated with high glucose (40 mM) and CBD (1 μ M and 5 μ M) over 48 (A) and 72 hours (B). * $p < 0.05$, ** $p < 0.01$, *** $p < 0.001$, and **** $p < 0.0001$. C, Control; G, glucose; LCBD, low CBD; HCBD, high CBD; LCBD+G, low CBD with glucose; HCBD+G, high CBD with glucose.

Figure 3.9. Concentrations of PDGF-BB cytokine in HepG2 cells treated with high glucose (40 mM) and CBD (1 μ M and 5 μ M) over 48 (A) and 72 hours (B). * $p < 0.05$, ** $p < 0.01$, *** $p < 0.001$, and **** $p < 0.0001$. C, Control; G, glucose; LCBD, low CBD; HCBD, high CBD; LCBD+G, low CBD with glucose; HCBD+G, high CBD with glucose.

LIST OF TABLES

Chapter 2

Table 2.1. Table indicating the exact volumes of each component in the master mix

Table 2.2. Forward and reverse sequences of primers

Table 2.3. Amount of each component for RT-PCR

Table 2.4. The following thermal cycling program was followed for the RT-PCR reactions. The annealing temperatures differed according to each target gene

Table 2.5. Annealing temperatures used for RT-PCR

Table 2.6. The components for the reverse transcription master mix

Table 2.7. qPCR cycling conditions

Table 2.8. The master mix quantities for RT-PCR of miRNA

Table 2.9. Thermal cycler program for miRNA

Table 2.10. Quantities used to dilute coupled beads to 1x in Bio-Plex buffer

Abbreviations

AGO2	Argonaute 2
ATP	Adenosine triphosphate
BCA	Bicinchoninic acid
CBD	Cannabidiol
CBN	Cannabinol
DGCR8	DiGeorge syndrome critical region 8
DM	Diabetes mellitus
DMEM	Dulbecco's Modified Eagle Medium
dsRBD	Double-stranded RNA binding domain
ECS	Endocannabinoid system
EC	Endogenous cannabinoids
ELISA	Enzyme-linked immunosorbent assay
FABP	Fatty acid binding protein
FBS	Fetal bovine serum
GABA-A	Gamma-aminobutyric acid type A receptor
GPR55	G-protein coupled receptor 55
IDF	International Diabetes Federation
IR	Insulin resistance
IL-10	Interleukin-10
IL-1 β	Interleukin 1 Beta
IL-12	Interleukin-12
IL-6	Interleukin-6
miRNA	MicroRNA
MAPK	Mitogen-activated protein kinase
Nrf2	Nuclear factor erythroid 2- related factor 2
NF- κ B	Nuclear factor kappa-light-chain-enhancer of activated B cell
PARP	Poly Adenosine Diphosphate-Ribose Polymerase

RISC.	RNA-induced silencing complex
RNAP III	RNA polymerase III
RNS	Reactive nitrogen species
ROS	Reactive oxygen species
THC	Tetrahydrocannabinol
TRBP.	Tar RNA binding protein
TRPV1	Transient receptor potential cation channel subfamily

CHAPTER ONE

Introduction and Literature Review

1.1 DIABETES AND INSULIN RESISTANCE

Diabetes mellitus (DM) is a range of metabolic disorders arising from issues with insulin action, insulin secretion, or a combination of both (Ozougwu, 2013). DM is characterised by a chronic hyperglycaemic condition. It was estimated by the International Diabetes Federation (IDF) that 456 million adults presented with diabetes in 2017. It is projected that there will be 693 million cases of diabetes by 2045 (Cho, 2018). Diabetes was initially documented by the ancient Egyptians about 3,000 years ago. The clear differentiation in relation to type 1 and type 2 diabetes was established in 1936 (Feng, 2016). Type 2 diabetes accounts for 90-95% of all diabetes cases (American Diabetes Association, 2012) and results from a reduced sensitivity of target tissues to insulin (Ozougwu, 2013). Age, minimal or no exercise, obesity, and a strong familial history of DM are some of the significant risk factors linked to the onset of type 2 DM (Fletcher, 2002). Type 2 DM is mediated by metabolic mechanisms (Eizirik, 2020), and the loss of beta cells is attributed as a key mechanism. Insulin resistance (IR) plays a crucial role in the onset of type 2 diabetes and is also involved in related metabolic issues, including dyslipidaemia and hypertension (Goldstein, 2002).

IR occurs when cells become unresponsive to the actions of insulin. Ultimately, the pancreas must produce larger amounts of insulin to elicit the same desired effect on cells. Eventually, the pancreas will not maintain this excessive production and insulin production will fail, generally progressing to type 2 DM (Stroppler, 2021). Insulin resistance is a strong predictor of future type 2 diabetes onset and becomes a treatment focus when hyperglycaemia is present (Taylor, 2012). There is an increased risk of DM if a patient presents with IR, and many people are insulin resistant for years without knowing it (Roland, 2014).

Lipids, proteins, and carbohydrates are all converted into glucose, which is in turn converted into adenosine triphosphate (ATP) at the cellular level. ATP functions as energy for cells, and is used to contract muscles, actively transport molecules across cell membranes, and perform mechanical work (Mihir, 2020). The liver influences glucose homeostasis by controlling pathways of glucose metabolism, including glycolysis, glycogenolysis and glycogenesis (Hans, 2016). The liver's metabolic activity is carefully regulated through insulin and other hormones (Rui, 2011). Understanding the typical processes of glucose metabolism in the liver is crucial for gaining insights into the underlying causes of diabetes mellitus. Additionally, liver glucose metabolism is closely linked to glycosylation reactions and interconnected with the metabolism of fatty acids. The liver receives dietary carbohydrates from the intestines via the portal vein.

Inside the hepatocyte, glucokinase converts glucose into glucose 6-phosphate, ensuring a steady supply of glucose for cellular metabolism. Glucose 6-phosphate can then enter various metabolic pathways. After a meal, the majority of glucose 6-phosphate (G6P) is directed toward glycogen synthesis, involving the creation of glucose 1-phosphate and UDP-glucose. Small amounts of UDP-glucose are diverted to produce UDP-glucuronate and UDP-galactose, which act as monosaccharide donors necessary for glycosylation (Adeva-Andany, 2016). Another metabolic pathway for glucose 6-phosphate leads to the synthesis of fructose 6-phosphate, which may either enter the hexosamine pathway to produce UDP-N-

acetylglucosamine or proceed through glycolysis to generate pyruvate and subsequently acetyl-CoA. When there is an abundance of glucose in the liver cell, acetyl-CoA can either participate in the tricarboxylic acid (TCA) cycle for oxidation or move to the cytosol for fatty acid synthesis (Adeva-Andany, 2016). Additionally, glucose 6-phosphate can generate NADPH and ribose 5-phosphate through the pentose phosphate pathway. This glucose metabolism provides intermediates for glycosylation, a post-translational modification essential for regulating the function of proteins and lipids. Congenital conditions with phosphoglucomutase (PGM)-1 and PGM-3 deficiencies are linked to impaired glycosylation. Beyond carbohydrate metabolism, the liver manufactures glucose for use by other tissues, either by breaking down glycogen or by synthesizing it *de novo*, primarily utilizing lactate and alanine (gluconeogenesis) (Adeva-Andany, 2016). Changes in fatty acid metabolism within fat, liver, skeletal muscle, intestine, and pancreas significantly contribute to the development of insulin resistance, disrupted glucose processing, and the occurrence of type 2 DM (Stinken, 2015). The stimulation of the peripheral endocannabinoid system has been observed in human obesity, leading to hepatic steatosis, lipogenesis, increased insulin resistance and adipogenesis (Horath, 2012).

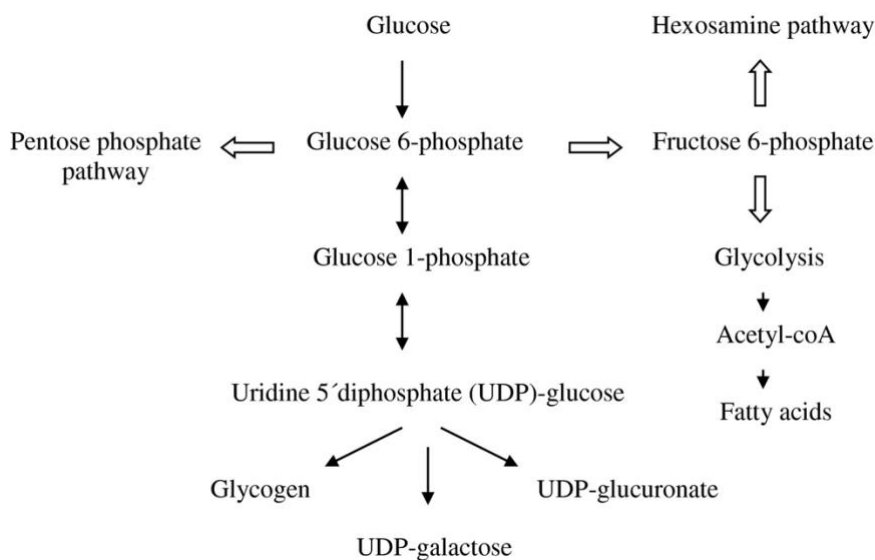


Figure 1.1. The metabolic processing of glucose in the human liver (Adeva-Andany, 2016).

1.2 THE ENDOCANNABINOID SYSTEM

In the early 1990s the endocannabinoid system (ECS) was identified (Petrocellis, 2004). Appearing early in evolution, the endogenous cannabinoid (EC) system is an abundant lipid signalling system, which has crucial regulatory roles throughout the body. Tiny molecules synthesized from anandamide, arachidonic acids, and 2-arachidonoylglycerol are the primary endocannabinoids. These endocannabinoids bind G-protein-coupled receptors, which are densely distributed in areas of the brain. This system is also one of the key regulators of the immune system, microcirculation, and autonomic nervous system (Rodriguez, 2005). Most components of the ECS are multifunctional. Rather than being an isolated system, the ECS influences and is influenced by many other signalling pathways (Lu, 2021).

Endocannabinoids are produced as needed from membrane phospholipids and are promptly

secreted by cells. Upon release, they bind to specific receptors to initiate a biological response, functioning in either a paracrine or autocrine manner (Baldassarre, 2013). These endocannabinoid molecules exert various effects on the central and peripheral systems, mainly via cannabinoid receptors CB1 and CB2 (Baldassarre, 2013). The ECS significantly influences inflammation, reactive oxygen species (ROS) production, and tissue injury (Horvath, 2012), and plays a role in numerous regulatory pathways in the human body, making this system a target for many therapies and drugs (Aizpurua-Olaizola, 2017). The ECS contributes to the regulation of glucose and lipid metabolism across multiple levels, resulting in the deposition of excess energy as adipose (Di Marzo, 2008).

A hyperactive ECS plays a role in diabetes development by encouraging lipid storage and increased energy intake, while disrupting lipid and glucose metabolism. It also promotes inflammation in pancreatic islets and apoptosis in pancreatic beta cells (Gruden, 2016). Increasing evidence suggests that the liver's glucose metabolism is partly regulated by the ECS, which is variably affected by insulin resistance and hepatic glucose metabolism.

Thus far, a minimum of two types of CB receptors have been discovered, namely CB1 and CB2. CB1 and CB2 receptors differ in their basic structure, their ligand-binding characteristics, and their methods of signal transmission. Both belong to a larger family of receptors that interact with guanine-nucleotide-binding proteins and traverse cell membranes seven times, referred to as heptahelical receptors. These CB receptors have an extracellular N-terminal domain with glycosylation sites, an intracellular C-terminal domain connected to a G protein complex, and seven hydrophobic transmembrane segments joined by alternating extracellular and intracellular loops. Researchers have developed and compared three-dimensional models to illustrate the arrangement of helices in CB1 and CB2 receptors across humans, rats, and mice (Svizenska, 2008). The ECS regulates renal homeostasis under normal conditions, while CB1 and CB2 receptors are essential in regulating renal function (Hryciw, 2016). CB1 receptors have been located in peripheral organs, including the liver (Chua, 2019), and studies have shown that CB1 receptors are upregulated during exposure to increased glucose levels in liver tissue (Chua, 2019). As more studies reveal the influence of the ECS on liver function, it is essential to interrogate the function of the liver and establish a link between the regulatory components of the ECS and liver function in maintaining systemic homeostasis.

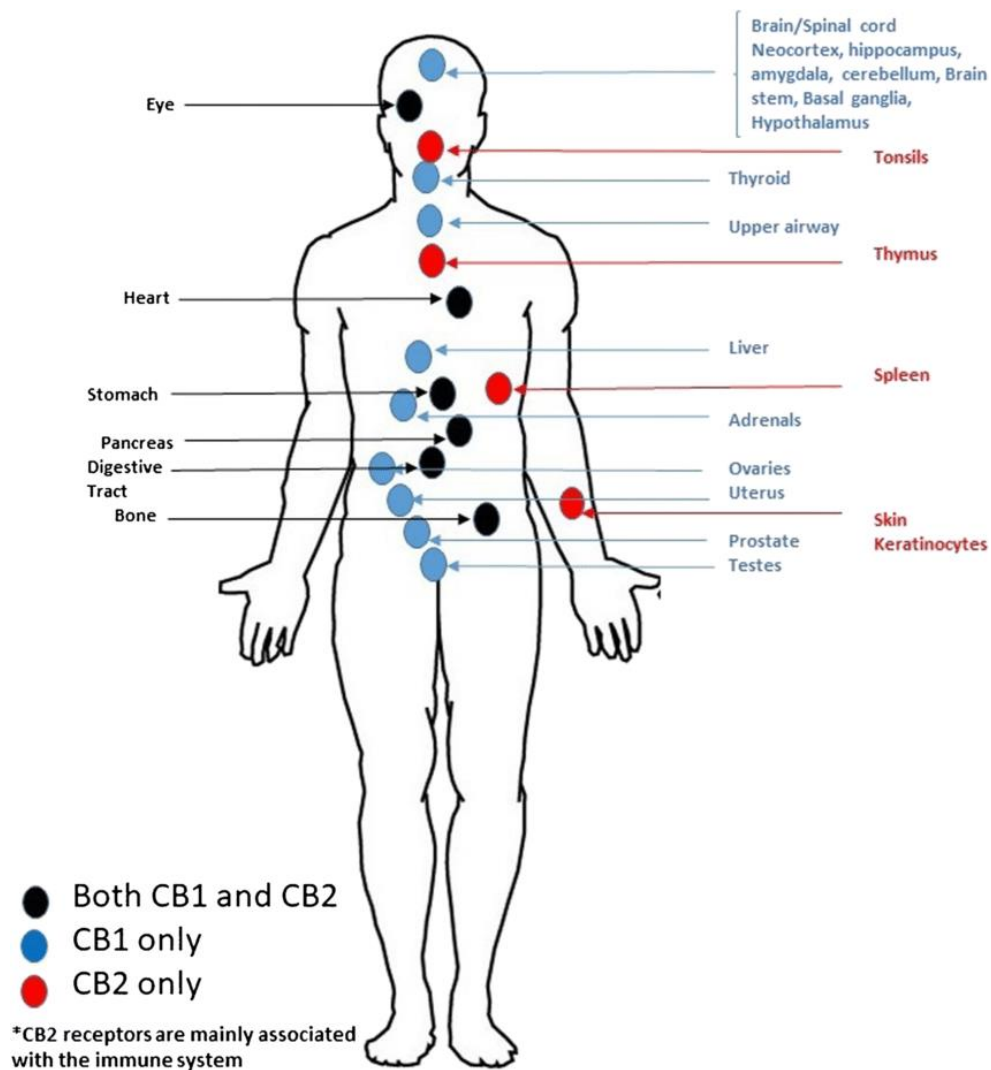


Figure 1.2. Location and distribution of CB1 and CB2 receptors in the human body (Muralidhar, 2019).

1.3 THE LIVER

Many foods and drugs affect the liver. The liver performs more than 500 roles in the human body, including bile production, blood volume regulation, and lipid and cholesterol homeostasis. The liver stores glucose during feeding in the form of glycogen via the gluconeogenic pathway. During fasting, the liver converts the glycogen back into glucose for the body to use (Trefts, 2017). In relation to nutrient intake and insulin secretion, the liver is placed centrally since both nutrients and insulin must pass through the liver (Figure 1). About 50% of insulin is extracted at first passage through the liver, which may be reduced in the insulin resistant liver. Increasing fat and carbohydrate intake may challenge the liver, which influences the net hepatic glucose balance and the degree of hepatic lipoprotein accumulation, which is linked to insulin resistance (Staehr, 2004). The liver is highly susceptible to reactive oxygen species (ROS) produced during metabolic activities, and experiences oxidative stress when there is a disturbance in the redox equilibrium. This oxidative stress impacts liver functionality, influences inflammatory pathways, and plays a role in disease progression (Allameh, 2023). Oxidative stress is a recognized factor in the development and advancement of diabetes. Impaired

glucose tolerance, beta cell dysfunction, and insulin resistance represent conditions induced by an oxidative environment, which may lead to a diabetic disease state (Rain, 2011).

1.4 OXIDATIVE STRESS PATHWAYS

Oxidative stress contributes to the development of DM (Maritim, 2003). The terms reactive nitrogen species (RNS) and ROS refer to free radicals and oxidants. Biological free radicals, which are highly unstable molecules, are generated through normal cellular metabolism. Free radicals, when present at elevated levels, can damage cellular structures, and at low levels free radicals act as a defence against infectious agents and aid in the maturation process of cellular structures (Oguntibeju, 2019). ROS are produced through various constitutively active oxidases and through the electron-transport chain, in small amounts (Xu, 2016). In DM, the oxidation of glucose, the oxidative degradation of glycated proteins, and the non-enzymatic glycation of proteins contribute to an overproduction of free radicals. A reduction in antioxidants, combined with elevated or abnormal levels of free radicals, results in cellular damage and dysfunction, potentially contributing to the development of insulin resistance (Maritim, 2003).

Excessive nutrient intake, episodes of ketosis, and sleep restriction can cause oxidative stress. Serine/threonine kinases, such as mitogen-activated protein kinase (MAPKs) and poly adenosine diphosphate-ribose polymerase (PARP), which have a negative effect on insulin signalling, are activated by oxidative stress (Rain, 2011). Oxidative stress can induce cellular dysfunction and lead to cell death. Apoptosis, a programmed cell death, functions to destroy damaged or potentially dangerous cells, such as tumour cells (BD Editors, 2017). Apoptosis occurs via two pathways, namely the extrinsic and intrinsic pathways. The mechanisms of these pathways are very sophisticated, complex, and involve an energy-dependent cascade of molecular events. Evidence suggests that the two pathways are interconnected, with molecules from one pathway influencing the other (Elmore, 2007). Caspase-8, -9, -12, -7, and -3 are usually involved in the caspase dependent pathway. Several receptors also play roles in this process, namely TNF- α receptors, Toll-like Receptors (TLRs), and death receptors. Regarding the caspase independent pathway, the mitochondrial membrane potential is altered, which in turn initiates the first step of apoptosis, which is mitochondrial damage. This increases ROS production, which further induces caspase-independent apoptosis. Hydrogen peroxide is a toxic by product of various metabolic reactions. Catalase, a vital antioxidant enzyme found in most aerobic organisms, is instrumental in converting two molecules of hydrogen peroxide into one molecule of oxygen and two molecules of water through a two-step process. The initial stage of the reaction mechanism entails the creation of a distinct intermediate compound known as "compound I" This compound is characterized by a covalently bonded oxyferryl species (FeIVO) with a porphyrin π -cation radical, achieved by the reduction of a single molecule of hydrogen peroxide. In the subsequent step, compound I undergoes reduction through redox reactions involving a two-electron transfer from an electron donor (which is the second molecule of hydrogen peroxide). This process results in the production of the unbound enzyme, along with oxygen and water (Nandi, 2019). Superoxide dismutase (SOD) is the initial detoxifying enzyme and the most potent antioxidant within the cell. This crucial endogenous antioxidant plays a pivotal role as part of the primary defence system against ROS. It facilitates the conversion of two molecules of superoxide anion (O_2^-) into hydrogen peroxide (H_2O_2) and molecular oxygen (O_2) through a process called dismutation. This effectively reduces the potential harm posed by superoxide anions. SOD is classified as a metalloenzyme, meaning

it relies on a metal cofactor to carry out its enzymatic activity (Ighodaro, 2018). GPx-1 is another vital antioxidant enzyme responsible for preventing the harmful build-up of hydrogen peroxide within cells. It is present in various cellular compartments, including the cytosol, mitochondria, and in some cases, peroxisomes. Under many physiological conditions, GPx-1 is reportedly more efficient than catalase in eliminating intracellular peroxides. The comparative efficacy of peroxiredoxins and GPx in regulating intracellular hydrogen peroxide levels has been a subject of discussion. While peroxiredoxins are highly expressed and exist in different isoforms within the cytosol and mitochondria, certain forms of peroxiredoxins are vulnerable to oxidative deactivation even at relatively low concentrations of hydrogen peroxide. Additionally, GPx-1 has the capability to reduce lipid hydroperoxides and other soluble hydroperoxides once they are released from membrane lipids. It may also have the capacity to reduce specific types of phospholipid-monoacylglycerol hydroperoxides, such as 1-linoleoyl Lys phosphatidylcholine hydroperoxide, but not tri- or diacylglycerol hydroperoxides (Lubos, 2011).

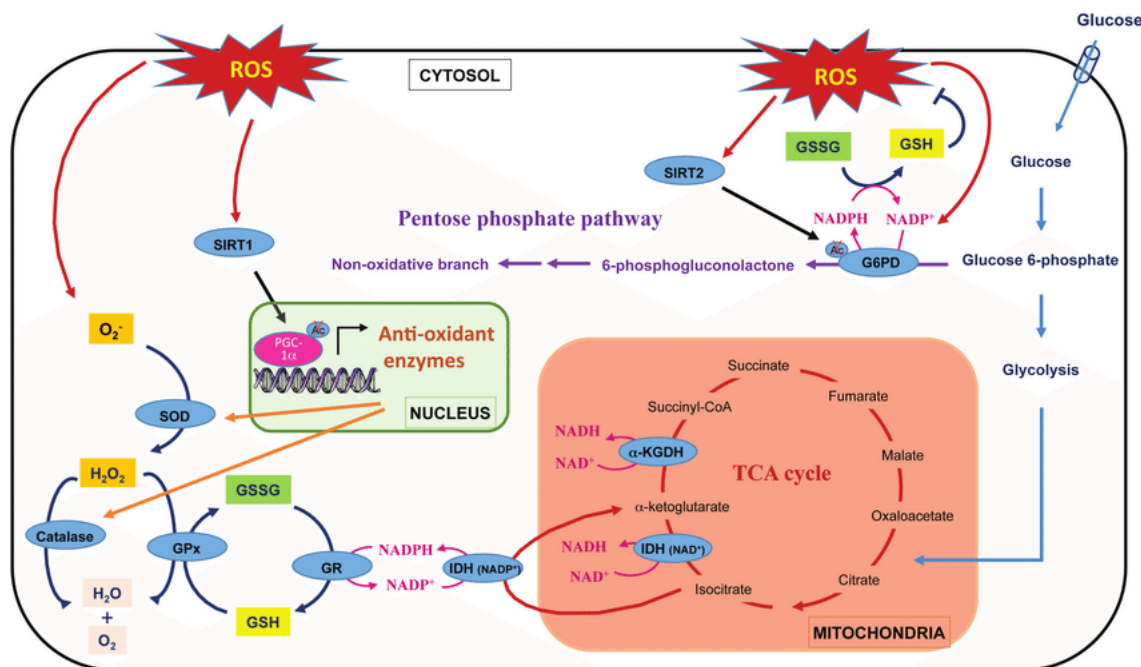


Figure 1.3. Redox cycles linking metabolic and antioxidant pathways (Mendez, 2017).

Peroxisome Proliferator Activated Receptors (PPARs) belong to the nuclear hormone receptor superfamily and possess functional domains typical of other superfamily members. Originally known as "orphan nuclear receptors," it is now recognized that PPARs can bind a variety of natural and synthetic ligands, acting as agonists, antagonists, or inverse agonists. Some of these ligands can stimulate peroxisome proliferation in rodent hepatocytes to different extents, leading to the identification of their receptors as PPARs. In humans, there are three distinct subtypes—PPAR α , β/δ , and γ —each encoded by separate genes and showing tissue-specific expression. The Peroxisome Proliferator Activated Receptors Gamma (PPAR γ) gene produces three different mRNA transcripts (γ 1, γ 2, γ 3). All subtypes play a role in regulating lipid and carbohydrate metabolism. Moreover, based on their expression in particular cell types or tissues, PPARs can significantly affect various cellular functions such as proliferation,

apoptosis, differentiation, as well as inflammatory processes, angiogenesis, and immune responses (Muzio, 2021).

Nuclear factor erythroid 2-related factor 2 (Nrf2) acts as the central controller in the transcriptional response of cells to oxidative stress. Nrf2 oversees the activation of various genes responsible for antioxidants and phase II enzymes. Nrf2 is regulated by Kelch-like ECH-associated protein 1 (Keap1), which serves as a connecting protein in the cytoplasm, allowing Nrf2 to be tagged with multiple ubiquitin molecules by the Cullin 3 (Cul3) E3 ubiquitin ligase, leading to its breakdown in the proteasome. This continuous degradation of Nrf2 ensures a low baseline level of expression in unstressed conditions. However, in the presence of oxidative stress, specific sulphur-containing amino acids in Keap1 are altered, causing a structural shift that prevents Keap1 from facilitating the ubiquitination of Nrf2 by Cul3. As a result, Nrf2 becomes more stable, accumulates, and moves into the nucleus, where it forms complexes with small Maf proteins and attaches to the antioxidant response element (ARE), promoting the robust activation of genes involved in cellular defence against ROS and other oxidative agents (Ngo, 2022). In situations of oxidative stress, complex molecular mechanisms, both in terms of gene expression and subsequent processing, establish a connection between Nrf2 and NF- κ B, and this interaction varies depending on the type of cell. When Nrf2 is deactivated, it heightens NF- κ B activity, thereby increasing cytokine production. Conversely, NF- κ B influences both the transcription and functioning of Nrf2. Cells lacking Nrf2 exhibit a more pronounced NF- κ B activity and an augmented function of IKK- β . Heme oxygenase-1 contributes to Nrf2's ability to hinder NF- κ B by reducing NF- κ B-driven transcription of adhesion molecules in endothelial cells. However, NF- κ B impedes Nrf2 by competing for the transcriptional co-activator CBP (CREB-binding protein)-p300 complex (Lingappan, 2018). The transcription factor HIF-1 α , in response to oxidative stress, orchestrates adaptive reactions by relocating to the cell nucleus and controlling gene expression. Alterations in mitochondria play a crucial role in this adaptive reaction to oxidative stress (Li, 2019).

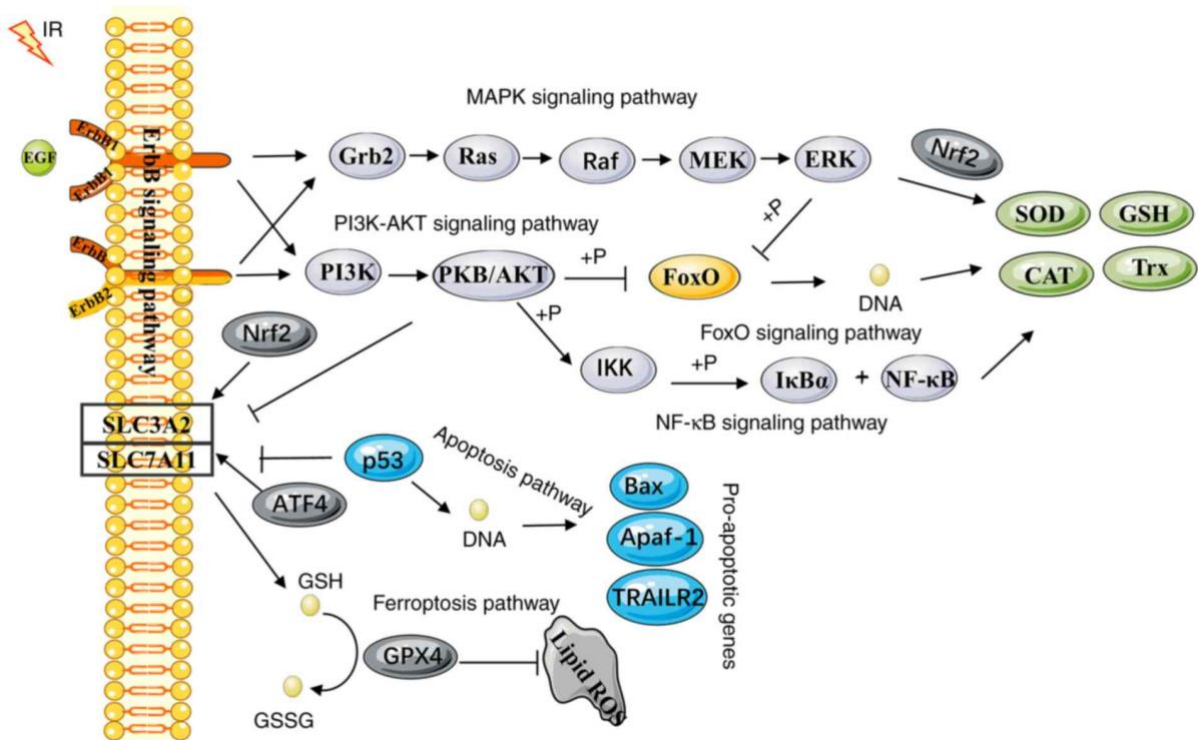


Figure 1.4. Different pathways and genes that are involved in oxidative stress (Liu, 2022).

1.5 CANNABIS AND CANNABINOID COMPOUNDS

One of the most consumed drugs worldwide is Cannabis, which is consumed by an estimated 200-300 million people (Concalves, 2019). Cannabis is one of mankind's oldest crops, and has been used as a source of food, fuel, and fibre for thousands of years. Specific compounds within cannabis plants may be used to ease pain, help with relaxation, and offer other benefits (Brewer, 2020). Cannabis was prescribed for many conditions in South Africa from the mid-19th century to the 1920s (Maule, 2015), and became a schedule 1 substance in 1928, which made it illegal and classified the drug as "without medical value" (Maule, 2015). Current research estimates that the global industrial hemp industry will expand from a \$4.41 billion market in 2018 to a \$14.67 billion market by 2026 (Brewer, 2020). Three main species of cannabis are recognised, namely *Cannabis sativa*, *Cannabis indica*, and *Cannabis ruderalis*. However, *Cannabis ruderalis* may fall under *Cannabis sativa*. Cannabis contains more than 545 known compounds (Goncalves, 2019), and 86 cannabinoid chemicals have been identified. The main psychoactive chemical is tetrahydrocannabinol (THC); other cannabinoid chemicals include cannabidiol (CBD) and cannabinol (CBN) (Fachetti, 2018).

Cannabinoids remain in the body for extended periods of time due to their high lipid solubility. THC remains within the body for up to 67 days in extreme chronic users and four days in occasional users, although THC is broken down in the liver into THC-COOH. Cannabis can be readily absorbed into the lipid membrane of neurons and other cells, and can effectively treat many health problems (Fachetti, 2018). No reports of fatal cannabis overdoses have been recorded in humans to date. This is due to the paucity of receptors in the medullary nuclei, which is the part of the brain that controls cardiovascular and respiratory functions (Farhat, 2011). CBD was first isolated from Mexican Marijuana in 1940 (Mechoulan, 2002), and its structure and stereochemistry were determined in 1963 (Booz, 2011). CBD has very

few psychoactive effects (Gonçalves, 2019), is the second most common cannabinoid found in cannabis, and has been found to work with THC to suppress pain. Unlike THC, CBD does not activate CB1 receptors in the brain and therefore does not exert psychotropic effects (Mattes, 2020). CBD is not rimonabant-like in its actions and thus appears very unlikely to produce unwanted central nervous system effects. Rimonabant was developed as an anti-obesity agent, which was withdrawn from the market due to adverse psychiatric side effects. Numerous studies involving both animals and humans indicate that blocking CB1 receptors (CB1R antagonism) is significantly beneficial in treating obesity, metabolic issues, and drug addiction. Nonetheless, rimonabant, the pioneering CB1R blocker and reverse activator, showed promise in treating obesity and aiding in quitting smoking, but was associated with severe mental health side effects, such as anxiety, depression, and thoughts of suicide, leading to its removal from the European market (Nguyen, 2019). CBD is a very low affinity CB1 ligand that can nevertheless affect CB1 receptor activity (McPartland, 2015). CBD has been shown to exert anti-inflammatory and anti-anxiety properties, as well as anti-aging properties for the skin (Fachette, 2018), and is usually well-tolerated without any intoxicating side effects (Grotenhermen, 2016). CBD is reportedly a potent antioxidant, which protects cells against chemical damage due to oxidation, and may play a role in protecting against the development of diabetes and certain types of cancer. The dosage response to CBD is biphasic, which means that efficacy is lost if the dose is too high or low (Farhat, 2011). THC binds mostly to CB1 and CB2 cannabinoid receptors. Co-ordination, time perception, memory, pleasure, and thought processes are affected when THC attaches to its receptors (Fachette, 2018). CB1 receptors are located primarily in the cerebral cortex and hippocampus, which control cognition and memory, respectively. CB2 receptors are mostly found in the arms and legs (extremities) and in immune tissues (Farhat, 2011). CBD exerts beneficial effects in a wide range of disorders, such as diabetes, cancer, and colitis (Stanley, 2013).

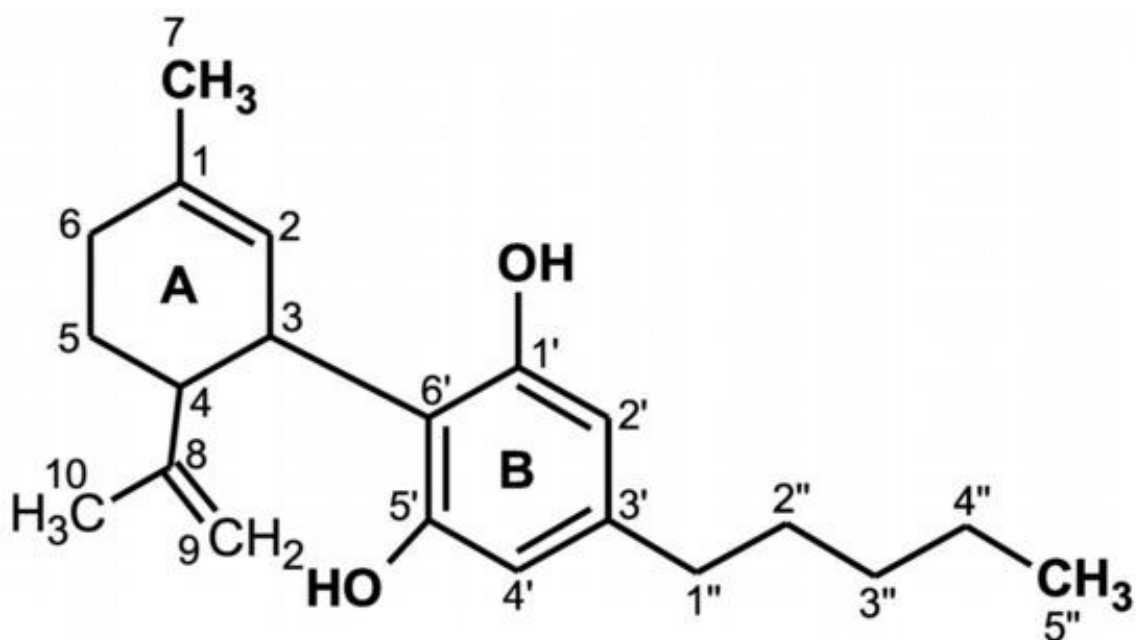


Figure 1.5. Chemical Structure of CBD (Atalay, 2019).

1.6 THE LAWS REGARDING CBD USE IN SOUTH AFRICA

Cannabis was introduced into South Africa when Indians were brought to work as labourers on the sugarcane plantations in Natal in the 1980s (Van Rensburg, 2020). The possession and personal use of cannabis was a criminal offense in South Africa. Commonly known as “dagga” in South Africa and marijuana in other countries. There were two Acts of Parliament that made cannabis illegal, the Drug and Drug Trafficking Act 140 of 1992 and the Medicines and Related Substance Control Act of 1965 (Lubaale, 2019). The South African Constitutional Court decriminalised possession, cultivation, and the use of cannabis in private by adults on the 18th of September 2019. The Act was deemed to be constitutionally invalid, and Parliament was required to revise the wording (Van Rensburg, 2020). The legalisation of cannabis in South Africa has led to increased use of cannabis and cannabis-related products in the country. Many individuals report beneficial effects; however, the exact mechanisms and actions of cannabis compounds are unclear.

1.7 THE EFFECTS OF CBD

As the perception of cannabis is shifting, it is important to understand the physiological and behavioural effects of the compound (Farokhnia, 2020). Cannabis use is associated with a 16% lower fasting glucose and a smaller waist circumference (Penner, 2013). CBD demonstrates anti-autoimmune properties and has been shown to rescue insulin forming cells from damage, thus promoting normal glucose metabolism (Fachette, 2018). Cannabinoids inhibit the release of several inflammatory mediators, some of which lead to DM (Alshaarawy, 2015). The ECS consists of G-protein coupled cannabinoid receptors, CB1 and CB2, found in both the central nervous system and peripheral tissues, along with arachidonate-derived lipid ligands like anandamide, and the enzymes responsible for synthesizing and breaking down these ligands. This system plays a role in various processes, such as pain sensation, mood, and appetite (Booz, 2011), and regulates energy homeostasis and food intake by activating cannabinoid receptors, which may reduce body weight in individuals suffering from type 2 DM (Mattes, 2020). A cross-sectional study conducted in the United States of America showed that heavy and light users of cannabis exhibited lower odds of developing type 2 DM when compared to non-users (Danielsson, 2016). Cannabis may lower fasting insulin levels and the risk of insulin resistance. While cannabis is often linked to an unhealthy lifestyle, research has indicated that cannabis use may lead to a lower body mass index and a reduced prevalence of obesity (Danielsson, 2016). CBD can protect the human body against vascular damage caused by high glucose levels, inflammation, or induction of type 2 DM, and reduces vascular hyper-permeability associated with disease conditions (Stanley, 2013). A study by Weiss et al. showed that the pro-inflammatory cytokine IL-12 was significantly decreased, while the anti-inflammatory cytokine IL-10 was significantly increased in CBD-treated non-obese diabetes-probed female mice (Weiss, 2008). One study found that CBD suppressed pro-inflammatory cytokines (IL-6 and TNF- α) released *in vitro* and induced a greater immunosuppressive effect on cytokines when higher doses of CBD were administered (Lisano, 2020). Therapeutic doses of CBD range from 0.5 mg/kg/per day to 20 mg/kg/per day. There are no negative effects on the liver if the recommended maximum dosage of 20 mg/kg/per day is used, as was observed in a study involving humans to determine the safety of various CBD doses (Ashton, 2021). CBD may further impact epigenetic modifications as a mechanism of action. Interestingly, CBD has been shown to upregulate certain microRNAs (miRNAs), such as miR-34a, which is involved in several pathways, including RB/E2F cell cycle and Notch DII 1 signalling pathways.

miRNA-34a is a redox sensitive miRNA, which regulates *Nrf2*-driven gene expression (Juknat, 2019).

1.8 miRNAs

MicroRNAs (miRNA) have become more important in diagnosis and detecting diseases in the human body. MicroRNA are small non-coding RNAs, which are essential for controlling gene expression (Rong, 2013). miRNA are usually 20-24 nucleotides in length (Krol, 2010) and are found in blood, body fluids, lipoprotein complexes, and microvesicles (Arroyo, 2011). In the human genome, more than 2000 miRNA have been identified to date. miRNA play roles in various biological and pathological processes, and disrupted miRNA levels correlate with several diseases, including DM. Functional miRNAs originate from longer precursor molecules, known as "mir," which are encoded by miRNA genes. These precursor molecules undergo two ribonuclease reactions. The process begins in the cell nucleus, where the primary transcripts (pri-mir) are long and feature a polyadenylated tail at the 3' end and a 7-methylguanosine cap at the 5' end (Lee, 2002). These transcripts, generated by RNA polymerase II, fold into stem loop structures, and are cleaved by a large microprocessor complex (500-650 kDa) composed of RNA polymerase III (RNAP III), Drosha, and a co-factor called DiGeorge Syndrome critical region 8 (DGCR8) (Gregory, 2004). This cleavage produces several precursor miRNAs (pre-mir). These pre-miRNAs, which are approximately 60-100 nucleotides long, possess a two-nucleotide extension that binds to exportin-5 and Ran-guanosine triphosphate (GTP), protecting the pre-miRNA from degradation and facilitating its transport from the nucleus to the cytoplasm (Guttler, 2011). The second ribonuclease reaction occurs in the cytoplasm and is performed by RNA polymerase II (Dicer), along with the double-stranded RNA binding domain (dsRBD) protein Tar RNA binding protein (TRBP) and protein activator of PKR (PACT). During this phase, the stem-loop structure is removed, producing a mature miRNA (designated as miR), which is about 22-25 nucleotides in length and has a two-nucleotide overhang at each 3' end.

After this process, two strands are formed: one is the mature guide miRNA, which becomes part of the functional centre of the RNA-induced silencing complex (RISC), while the other, the passenger miRNA, is degraded (Sand, 2011). The naming convention for miRNAs includes sequential numerical identifiers and species-specific prefixes (e.g., hsa-miR for Homo sapiens and mmu-miR for mice). Paralogous sequences that vary by a few positions receive lettered suffixes (e.g., hsa-miR-200c), and distinct hairpin loci that produce identical mature miRNAs are assigned numbered suffixes (e.g., hsa-miR-10-1). The two mature strands may originate from opposite arms of the same hairpin precursor and are indicated by the suffixes 5p or 3p, denoting their source (Griffith-Jones, 2006). Mature miRNAs recognize their target messenger RNAs (mRNAs) through complementary base pairing between nucleotides 2-8 at the 5' end (known as the seed region) of the miRNA and corresponding nucleotides in the 3' untranslated region (3' UTR) of mRNAs, which is essential for miRNA function (Kuhn, 2008). The miRNA/RISC complex, along with Argonaute 2 (AGO2), binds to the 3' UTR of the target mRNA (Wang, 2009). This results in the miRNA/RISC complex base pairing with the mRNA, leading to mRNA degradation if there is complete complementarity, or causing translational repression in cases of partial complementarity (Reinhart, 2000).

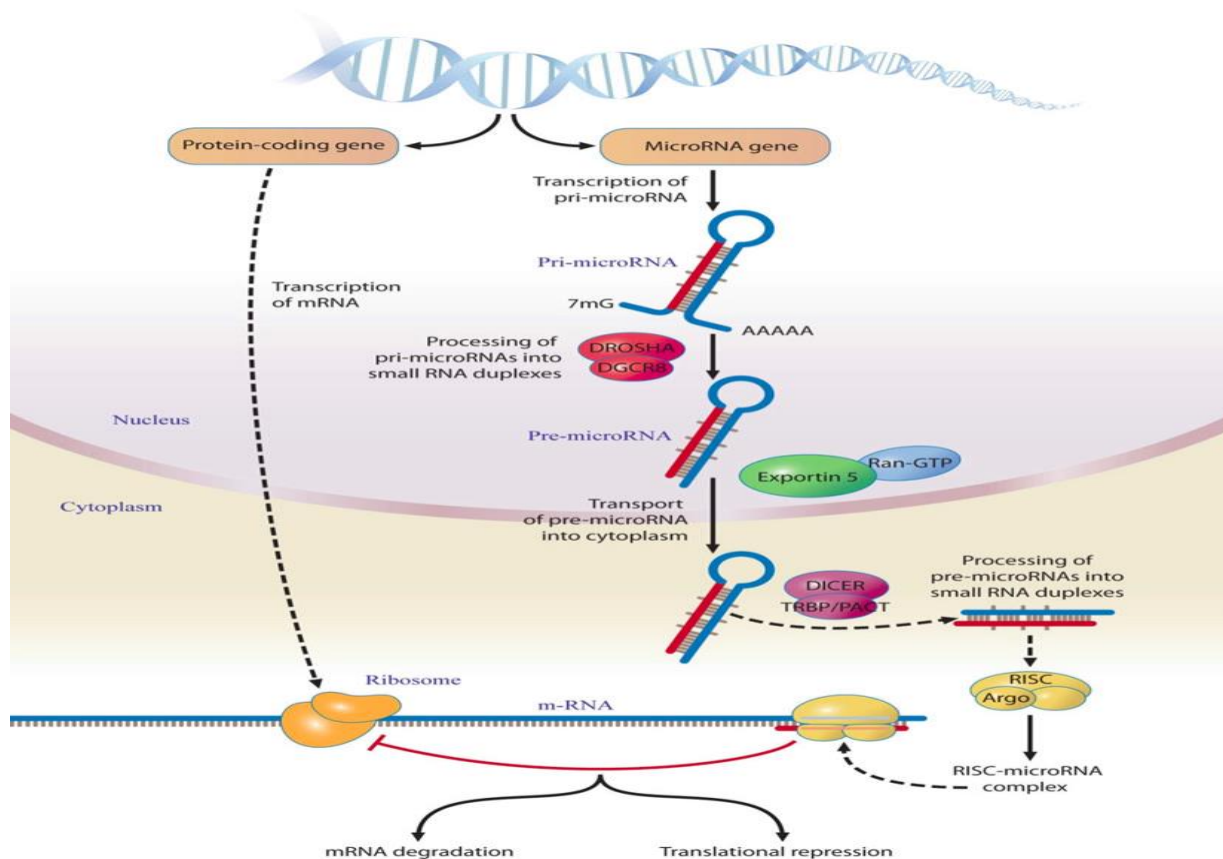


Figure 1.6. The miRNA formation process involves two maturation stages driven by the RNase enzymes Dicer and Drosha. The initial step occurs within the nucleus, while the subsequent step occurs in the cytoplasm, resulting in the creation of two distinct miRNA strands. The mature guide strand derived from this process can execute either translational repression or mRNA degradation functions (Sand, 2014).

The pathogenesis of DM is affected by miRNA that influence pancreatic beta-cell functions, insulin resistance, or both (Feng, 2016). miR-143, miR-103, and miR-107 display strong associations with type 2 DM (Chakraborty, 2014). miR-103 plays a role in regulating glucose homeostasis in type 2 DM (Luo, 2020). In metabolic diseases, the link between miR-107 expression levels, insulin resistance, and inflammation may be crucial, while reduced miR-107 levels may limit insulin resistance (Foley, 2012). However, miR-143 is upregulated in the liver and disrupts insulin-stimulated AKT activation and glucose homeostasis (Jordan, 2011). miRNAs may play important roles in understanding insulin resistance, DM, and the progression of diabetes- and obesity-related diseases. Investigating and understanding how miRNA expression influences gene and protein expression may hold the key to novel treatments for diabetes. miRNA-21, a multipotent miRNA, which promotes cell proliferation, immune destruction, and inflammation (Tang, 2019), is ubiquitous in several organ systems, including the heart, kidneys, small intestines, and spleen (Li, 2013). miRNA-21 is linked to prediabetic conditions and shows potential as a predictor for the early identification of glucose imbalances (La Sala, 2019).

1.9 STUDY RATIONALE

The South African healthcare system is increasingly burdened with cases of non-

communicable diseases. Thus, it is essential to identify innovative methods to treat or prevent DM and related illnesses. CBD has been illegal in most countries for many years, therefore very little research has been conducted on the compound in relation to human health. CBD has recently become legal in South Africa and many South Africans currently use CBD in various formulations, including oils, creams, tinctures, and edible items, for many different reasons. Therefore, further research should be conducted in order to understand the compound and its functions in the human body. CBD displays many promising effects, such as anti-inflammatory and antioxidant properties, exerts minimal psychoactive effects, and is not addictive. As such, CBD may provide a promising alternative therapeutic option and may be useful in treating type 2 DM.

1.10 AIMS AND OBJECTIVES

1.10.1 AIM

To investigate the effects of CBD on high glucose conditions in an *in vitro* liver model.

1.10.2 OBJECTIVES

- Investigate the effects of CBD on human liver HEPG2 cells over a 48 and 72 hour time period.
- The effect of CBD on oxidative stress/antioxidant response over a 48 and 72 hour time period.
- Identify if CBD affects miRNA-34a expression in cells exposed to high glucose levels.
- Determine the effects of CBD on the HIF1A gene associated with glucose homeostasis.
- Determine if CBD influences cytokines/proteins associated with inflammation.

1.11 HYPOTHESIS

It is hypothesised that CBD will alter the miRNA profile and ameliorate any negative effects associated with high glucose conditions, such as increased oxidative stress or inflammation.

CHAPTER TWO

METHODOLOGY

2.1 MATERIALS

Trypsin, Trypan Blue, glucose, chloroform, isopropanol, ethanol, and cell culture flasks were purchased from Sigma Aldrich (St Louis, MO, USA). Cannabidiol was kindly donated by GES Labs (Cape Town, South Africa). Trizol reagent and miRNA extraction and analysis kits were purchased from Qiagen (Hilden, Germany). The cDNA Synthesis Kit, Real Time PCR SSoAdvanced Kit and the Bio-Plex Pro Human Cytokine Assay was purchased from Bio-Rad (Hercules, CA, USA). Eagles' minimum essential media (EMEM) was purchased from Gibco, Thermo Fisher Scientific (Waltham, MA, USA). HepG2 liver cells were kindly donated by Prof JL Marnewick (Cape Peninsula University of Technology, South Africa).

2.2 METHODS

2.2.1 STUDY DESIGN

The glucose and CBD concentrations were selected based on previous literature. In this study, 40 mM glucose was used to establish high glucose conditions (Chu, 2011; Varma, 2005). Two CBD concentrations were used: low (1 μ M) and high (5 μ M) (Pagano, S, 2020; Kappor, 2012). Cells were categorized into six different treatment groups: 1) Control (normal complete culture medium (CCM)), 2) High glucose (normal CCM with 40 mM glucose), 3) Low CBD (normal CCM with 1 μ M CBD), 4) High CBD (normal CCM with 5 μ M CBD), 5) Low CBD with glucose (normal CCM with 1 μ M CBD and 40 mM glucose), and 6) High CBD with glucose (normal CCM with 5 μ M CBD and 40 mM glucose). Each treatment group was then exposed to the appropriate treatments for 48 and 72 hours.

2.2.2 CELL CULTURE

Cell culture involves laboratory techniques that allow eukaryotic or prokaryotic cells to grow in controlled environments. Its origins trace back to the early 20th century, where it was first employed to investigate tissue growth, virology, vaccine production, genetic factors influencing health and disease, and biopharmaceutical manufacturing through hybrid cell lines (Jedrzejczak-Silicka, 2017).

The application of cultured cells in experimental research is extensive, owing to the diverse range of cell types that can be propagated *in vitro*. In clinical research, cell culture is principally utilized to establish model systems for studying core aspects of cell biology, replicating disease processes, and evaluating drug toxicity. A significant advantage of cell culture is the capacity for precise manipulation of genes and molecular pathways. Additionally, the uniformity of clonal cell populations and the use of carefully controlled culture conditions minimize genetic and environmental variability, resulting in more reproducible and reliable outcomes compared to studies involving whole organisms (Segeritz, 2017).

Numerous studies have utilized the HepG2 cell line as an *in vitro* model for investigating hyperglycaemia (Chandrasekaran, 2010; Shokrzadeh, 2016; Zhou, 2021). These cells are widely recognized for their reliability, ease of culture, and well-defined characteristics. HepG2 cells were cultured in monolayer (1 million cells per flask) using Dulbecco's Modified Eagle Medium (DMEM) supplemented with 10% foetal bovine serum (FBS), 1% combination of penicillin, streptomycin, and fungizone (PSF), and 1% L-glutamine in 25 cm³ culture flasks. The culturing process occurred in a humidified chamber maintained at 37 °C with 5% CO₂. Cells were washed with phosphate-buffered saline (PBS) at a concentration of 0.1 M phosphate. When the cells reached a confluence level between 70-80%, the treatments were introduced into the cell culture vessels. The cells were then detached using trypsin, a proteolytic enzyme that cleaves at the C-terminal side of lysine and arginine. This process breaks down proteins that adhere to the vessel, facilitating easy resuspension during cell harvesting. Cell numbers were evaluated using the trypan blue exclusion method. Trypan blue is a dye used to count live cells by selectively staining dead ones. Live cells possess intact cell membranes, preventing trypan blue from penetrating and entering the cytoplasm. In contrast, dead cells have compromised membranes that enable the dye to enter the cytoplasm (Kumar, 2021). To prepare for cell counting, the cell suspensions were diluted at a 1:5 ratio by mixing 60 µL of CCM with 20 µL of the cell suspension and 20 µL of trypan blue. This mixture was then incubated for 5 minutes (min) at room temperature. A 22 × 22 cm coverslip was positioned on a sanitized hemocytometer, and 10 µL of the thoroughly combined solution was then applied to the haemocytometer. The living cell count was ascertained under a microscope utilizing the formula: (Average of live cells x 5 (for dilution) x 10,000).

2.2.3 RNA ISOLATION

RNA isolation involves the extraction of high-quality RNA from biological samples, enabling the study of gene expression and regulation. The principle of RNA isolation revolves around the disruption of cells and tissues, followed by the separation of RNA from DNA, proteins, and other cellular components using various methods, such as organic extraction or silica-based column purification (Wang, 2008). Maintaining the integrity and purity of isolated RNA is essential for downstream applications like reverse transcription PCR (RT-PCR), RNA sequencing, and transcriptomic analysis, as it directly influences the accuracy and reliability of experimental outcomes.

RNA Extraction

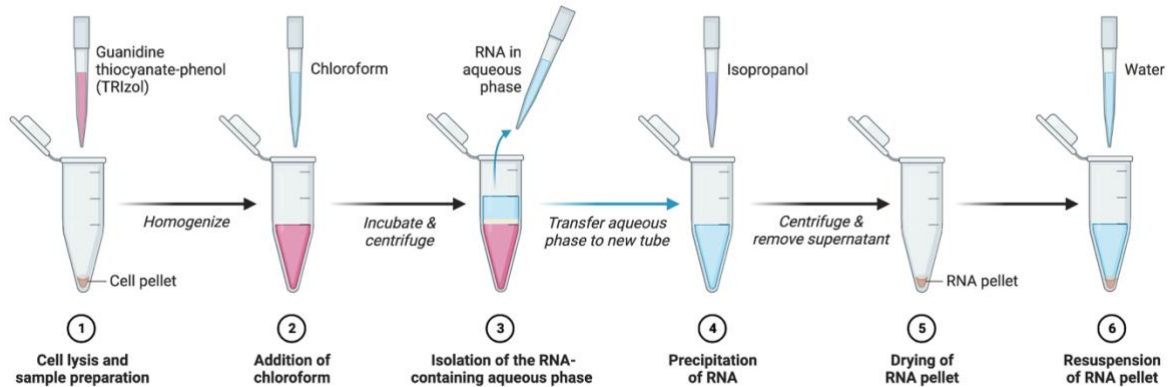


Figure 2.1. The extraction method used for RNA isolation (<https://www.addgene.org/protocols/kit-free-rna-extraction/>).

RNA isolation was performed using a previously published, optimized protocol for mammalian cells (Raghubeer et al. 2015). An equal volume of PBS and Trizol was introduced into the flask (500 μ l each), which was then incubated at room temperature for two minutes. Trizol is utilized because it preserves RNA integrity while lysing cells and dissolving their components. Next, a cell scraper was used to remove cells from the flask surface, which further introduces a physical method of disrupting the cells to release the RNA, collected into a microcentrifuge tube, and stored at -80°C overnight. Following an overnight incubation, the samples were thawed, and 100 μ l of chloroform was added to each tube. Chloroform, a critical reagent in RNA purification, facilitates phase separation, ensuring effective isolation of RNA from DNA and proteins. After vigorous shaking for 15 seconds (s), the tubes were incubated at room temperature for 2-3 min. Following this, centrifugation took place at 4°C at $12,000 \times g$ for 15 min. The resulting aqueous phase was carefully transferred to a new tube, and the work continued on ice to avoid degradation of the RNA.

Afterward, 250 μ l of isopropanol was added to each tube, which were then gently mixed and left to incubate overnight at -80°C . The role of the isopropanol is to precipitate the RNA, since RNA is insoluble in alcohols. Subsequently, the samples were thawed and centrifuged at 4°C at $12,000 \times g$ for 20 minutes. The supernatant was discarded, leaving the pellet. 500 μ l of cold 75% ethanol was used to wash the pellet, and after flicking to loosen the pellet, centrifugation was carried out at 4°C and $7400 \times g$ for 15 min. The ethanol was carefully removed without disturbing the pellet. The samples were allowed to air dry under a fume hood for 1-1.5 hours. Subsequently, the pellet was reconstituted in 15 μ l of nuclease-free water. The samples were incubated on ice for 30 min and then briefly incubated at room temperature for 2-3 min. After flicking the tubes to mix the contents, all tubes were placed on ice. RNA quantification was performed using the Nanodrop One (Thermo Fisher Scientific).

2.2.4 RNA QUANTIFICATION AND STANDARDISATION

To initiate RNA quantification using the NanoDrop One, the NanoDrop software was opened, and "New Workbook" was selected. The "RNA sample" option was chosen, and the device was blanked by applying 1 μ L of nuclease-free water (NFH₂O) to the sensor and gently closing it. The sensor was wiped carefully with a lint-free tissue. Then, 1 μ L of each RNA sample was added onto the sensor in a drop-wise manner. The samples were measured, and the concentrations and A260/280 values were recorded. The data was exported, and the results were documented. The NanoDrop concentrations were employed to standardize the RNA to 1000 ng in 10 μ L, ensuring consistent measurements and analysis.

2.2.5 cDNA SYNTHESIS USING THE iSCRIPT cDNA SYNTHESIS KIT

cDNA synthesis is a fundamental method in molecular biology that entails the reverse transcription of mRNA to create complementary DNA (cDNA), enabling the study and manipulation of gene expression. This process utilizes reverse transcriptase enzymes to generate a stable, single-stranded DNA template from mRNA, which can then be amplified and analysed using various downstream applications, such as PCR and sequencing (Ozsolak, 2011). The principle of cDNA synthesis is fundamental for converting the transient and fragile mRNA molecules into a more durable DNA form, thereby facilitating the exploration of transcriptomics, functional genomics, and the identification of novel gene sequences (Ozsolak, 2011).

A master mix was prepared, which included the 5 \times iScript reaction mix, reverse transcriptase, and NFH₂O. Table 2.1 indicates the exact volumes used for each reaction.

Table 2.1. Table indicating the exact volumes of each component in the master mix.

Reaction Component	Volume
5 \times iScript reaction mix	60 μ l
iScript reverse transcriptase	15 μ l
Nuclease-free water	210 μ l
RNA template	1 μ l

The master mix (19 μ L) and each standardized RNA sample (1 μ L) were added to a respective well in a 96-well PCR plate. The reaction protocol was executed following the instructions in the kit. After the PCR run was completed, the cDNA was pipetted into microcentrifuge tubes, and 80 μ L of NFH₂O was added to each tube. cDNA samples were stored at -20 $^{\circ}$ C and utilized for qPCR experiments.

2.2.6 REAL TIME PCR FOR GENE EXPRESSION USING BIO-RAD SSOADVANCED UNIVERSAL SYBR GREEN SUPERMIX

Real-Time PCR, also known as quantitative PCR (qPCR), is a sophisticated technique that amplifies and simultaneously quantifies a targeted DNA molecule, enabling the precise measurement of DNA or RNA levels in a sample. This method hinges on the use of fluorescent

markers, which emit a signal proportional to the amount of amplified product, allowing for real-time monitoring of the reaction as it progresses. The key principle of real-time PCR lies in its ability to provide both qualitative and quantitative data through the continuous collection of fluorescence emission during each cycle of the PCR process, facilitating high-throughput analysis and accuracy in gene expression studies, pathogen detection, and genetic variation analysis (Loftis, 2012). The SsoAdvanced Universal SYBR green protocol from Bio-Rad was followed. The SsoAdvanced Universal SYBR Green Supermix was brought to room temperature, thoroughly mixed, and briefly centrifuged to gather the contents at the bottom of the tubes. It was then placed on ice and shielded from light. A master mix was prepared and incubated on ice until use. Table 3 indicates each component of the qPCR master mix.

Primers for the study were sourced from Inqaba Biotechnical Industries (Pty) Ltd. Table 2.2 below presents the primer sequences of each gene. GAPDH was employed as the housekeeping gene in this assay, with three technical replicates per treatment.

Table 2.2. Forward and reverse sequences of primers

Gene	Forward sequence	Reverse sequence
<i>GPX1</i>	5'AAGGTGCTGCTCATTGAGAATG 3'	5'CGTCTGGACCTACCAGGAACTT 3'
<i>CAT</i>	5'ACGAGATGGCACACTTTGACAG 3'	5'TGGGTTTCTCTTCTGGCTATGG 3'
<i>SOD</i>	5'AGGATTAAGTGAAGGCGAGCAT 3'	5'TCTACAGTTAGCAGGCCAGCAG 3'
<i>NRF2</i>	5' AGTGGATCTGCCAACTACTC 3'	5'CATCTACAAACGGGAATGTCTG 3'
<i>HIF1A</i>	5'GAACGTCGAAAAGAAAAGTCTCG 3'	5' CCTTATCAAGATGCGAACTCACA 3'
<i>PPARG</i>	5' GGGATCAGCTCCGTGGATCT 3'	5'TGCACTTTGGTACTCTTGAAGTT 3'
<i>GAPDH</i>	5' TCCACCACCCTGTTGCTGTA 3'	5' ACCACAGTCCATGCCATCAC 3'

Table 2.3. Amount of each component for RT-PCR

Component	Volume per 10 μ l Reaction	80 wells
SYBR	5 μ l	400 μ l
Forward primer	0,5 μ l	40 μ l
Reverse primer	0,5 μ l	40 μ l
cDNA	1,5 μ l	*Added to each well separately
dH ₂ O	2,5 μ l	200 μ l

The reaction mixture was homogenized and 8 μ L of the master mix was aliquoted into each well of the qPCR plate. Then, 1.5 μ L of cDNA sample was added to each well containing the master mix. The plate was sealed with an optical transparent film, and thermal cycling was programmed as outlined in Table 2.4 for a total of 40 cycles.

Table 2.4. The following thermal cycling program was followed for the RT-PCR reactions. The annealing temperatures differed according to each target gene.

Step	Temperature	Time
Polymerase Activation and DNA Denaturation	95	4 min
Denaturation	95	15 sec
Annealing and extension	Determined by specific gene (Table 2.5)	40 sec
Melt Curve Analysis	72	30 sec

Table 2.5. Annealing temperatures used for RT-PCR.

Genes	Annealing Temperature (°C)
<i>CAT</i>	60
<i>SOD</i>	60
<i>GPX</i>	59
<i>NF-KAPPA BETA</i>	58
<i>NRF2</i>	55
<i>HIF1A</i>	55
<i>PPARG</i>	55

The qPCR plate was loaded into the QuantStudio 7 Flex (Life Technologies, USA) and the PCR run was started. Once the run was completed, the results were interpreted using the comparative critical threshold ($\Delta\Delta C_t$) method (Livak, 2001).

2.2.7 MICRORNA EXTRACTION

MicroRNA (miRNA) extraction is a crucial process in molecular biology aimed at isolating small, non-coding RNA molecules from biological samples, which play significant roles in gene regulation. The principle of miRNA extraction involves the selective purification of these short RNA sequences, often using techniques that exploit their size and unique chemical properties, such as silica-based column chromatography or organic extraction methods. Accurate extraction of miRNA is essential for downstream applications, including qPCR, microarray analysis, and next-generation sequencing, as it ensures the integrity and purity of the miRNA, thereby facilitating reliable studies of their expression profiles and functional roles in various biological processes and diseases (Ying, 2008).

The manufacturer's instructions were followed for miRNA isolation and analysis. miRNA was purified from a cell line that was rich in RNases; therefore prior to use, 10 μ L of beta-mercaptoethanol was incorporated into 1 mL of RLT buffer. Next, 260 μ L of RLT buffer was added to the pellet and vortexed for 30 seconds. Then, 80 μ L of buffer AL was added, mixed well, and incubated at room temperature for 3 minutes. The homogenized lysate was transferred to a gDNA eliminator spin column placed in a 2 mL collection tube, which was subsequently centrifuged at $\geq 8000 \times g$ for 30 seconds. The column was discarded, and the flow-through was retained.

Afterward, 1 mL of isopropanol was added and homogenized by repeated pipetting. The entire sample was subsequently transferred to the RNeasy mini column and centrifuged at $\geq 8000 \times g$ for 15 seconds, with the flow-through discarded. Next, 700 μ L of buffer RWT was added to the RNeasy mini spin column, which was centrifuged at $\geq 8000 \times g$ for 15 seconds, and the flow-through was discarded.

Next, 500 μL of buffer RPE was added to the RNeasy mini spin column, followed by centrifugation for 15 seconds at $\geq 8000 \times g$, after which the flow-through was discarded. Then, 500 μL of 80% ethanol was added to the RNeasy mini spin column and centrifuged for 2 minutes at $\geq 8000 \times g$. The flow-through and collection tube were discarded, and the RNeasy mini column was transferred to a new 2 mL collection tube. With the spin column lid closed, it was centrifuged at maximum speed for 1 minute to dry the membrane, discarding the flow-through and collection tube afterward. Finally, the RNeasy mini spin column was transferred to a new 1.5 mL collection tube. To elute the RNA, 30-50 μL of RNase-free water was gently added to the centre of the spin column membrane and incubated for 1 minute. The lid was then closed, and the column was centrifuged at maximum speed for 1 minute.

2.2.8 cDNA Synthesis

All reactions were performed on ice to minimize the risk of RNA degradation. The template RNA and 5x miRCURY RT reaction buffer were thawed on ice, whereas the RNase-free water was allowed to thaw at room temperature (15-25 $^{\circ}\text{C}$). Just before use, the 10x miRCURY RT enzyme was taken out of the freezer. Each solution was mixed by flicking the tubes, followed by a brief centrifugation to collect any remaining liquid from the tube walls, and kept on ice throughout the procedure.

80 μL of nuclease-free water was added to the tube to resuspend the UniSp6 RNA spike-in. It was mixed using a vortex and then briefly centrifuged. The tubes were incubated on ice for 20-30 minutes to ensure complete dissolution of the RNA spike-in. After this, the solution was mixed again by vortexing and spun down. Aliquots were stored at -30 to -15 $^{\circ}\text{C}$. Each template RNA was adjusted to the desired concentration using the formula $C_1V_1=C_2V_2$. The reverse transcription master mix was prepared on ice as per Table 2.6, thoroughly mixed, and kept on ice.

Table 2.6. The components for the reverse transcription master mix

Component	miRCURY LNA miRNA PCR Assay
5x miRCURY RT Reaction Buffer	30 μL
RNase-free water	67,5 μL
10x miCURY RT Enzyme Mix	15 μL
Synthetic RNA spike-ins	7,5 μL
Template RNA (5 ng/ μl)	2 μL

A total of 8 μL of master mix was dispensed into each well, followed by the addition of 2 μL of RNA, yielding a final reaction volume of 10 μL per well. The PCR assay was then performed according to the cycling conditions specified in the Table 2.7.

Table 2.7. qPCR cycling conditions

Step	Time	Temperature
Reverse transcription	60 minutes	42 °C
Inactivation of reaction	5 minutes	95 °C
Storage	Indefinite	4 °C

2.2.9 REAL-TIME PCR USING THE MIRCURY LNA SYBR GREEN PCR KIT

The miRCURY LNA miRNA PCR Assay was prepared by centrifuging the tube before its first opening. Next, 220 µL of nuclease-free water was added, and the tube was allowed to incubate at room temperature for 20 minutes. Following this, the reagents were vortexed. The template cDNA, Master Mix, primer set, RNase-free water and ROX Reference Dye were thawed and combined as indicated in Table 2.8. The cDNA was diluted 60-fold by adding 180 µL of RNase-free water to 20 µL of the RT reaction mix just before use, resulting in a mixture of 1 µL of cDNA and 59 µL of RNase-free water. A reaction mix was then prepared as indicated in the table below. Because of the hot start nature of the PCR reaction, it was unnecessary to keep samples on ice during the setup or while programming the real-time cycler.

Table 2.8. The master mix quantities for RT-PCR of miRNA

Components	miRCURY LNA miRNA PCR Assay
2x miRCURY SYBR Green Master Mix	200 µl
ROX Reference Dye	20 µl
PCR Primer Mix	40 µl
RNase-free water	20 µl
cDNA template	3 µl (60xdiluted)

The reaction was mixed thoroughly by vortexing and 7 µl was pipetted into each well of the PCR plate. Thereafter, 3 µl of the sample was pipetted into each well of the PCR plate. The real-time cycler was programmed according to the details in Table 2.9.

Table 2.9. Thermal cycler program for miRNA

Step	Time	Temperature
PCR initial heat activation	2 min	95 °C
Denaturation	10 s	95 °C
Combined annealing/extension	60 s	56 °C
Number of cycles	40*	
Melting curve analysis	60-95 °C	

The plate was placed in the cycler and the program was started. Once the run had completed, the results were interpreted.

2.2.10 BIO-PLEX PRO HUMAN CYTOKINE ASSAY

The principle behind these 96-well plate-formatted, bead-based assays resembles that of a capture sandwich immunoassay. In this process, an antibody specific to the target protein is covalently bound to internally dyed beads. These coated beads are then exposed to a sample containing the target protein, allowing a reaction to occur (Bio-Rad). The plate layout was meticulously planned prior to the experiment. The Bio-Plex Immunoassay System was initiated and allowed to warm up for 30 minutes. Meanwhile, wash buffer, the diluents, assay buffer, detection antibody diluent, standard diluent, and sample diluent were brought to room temperature, while all other reagents were kept on ice until needed. To ensure uniformity, all solutions were mixed by inversion to guarantee that all salts were fully dissolved. A 1x wash buffer was prepared by diluting 60 mL of the 10x wash buffer with 540 mL of distilled water. Frozen samples were taken out of storage and allowed to thaw at room temperature. The Bio-Plex System was calibrated using the Bio-Plex Manager Software. Controls and standards were reconstituted by adding 250 µL of standard diluent to each vial and vortexing at medium speed for 5 seconds. The vials were then incubated on ice for exactly 30 minutes. A four-step dilution series of standards and a blank were prepared, with each transfer followed by vortexing at medium speed for 5 seconds. The coupled beads were vortexed at medium speed for 30 seconds and then diluted to 1x in Bio-Plex buffer according to the dilution scheme outlined in Table 2.10. The beads were shielded from light by covering the containers with foil.

Table 2.10. Quantities used to dilute coupled beads to 1x in Bio-Plex buffer.

Number of wells	10x Beads, µl	Assay Buffer, µl	Total volume, µl
96	570	5130	5700

The diluted (1x) beads were vortexed to ensure consistency and 50 µL of the bead suspension was added to each well of the assay plate. The plate was washed twice with 100 µL of Bio-Plex buffer. Standards, samples, blanks, and controls were vortexed to ensure

thorough mixing, and 50 μL of each was transferred to the appropriate wells. The plate was sealed with tape and incubated on a shaker at 850 ± 50 rpm at room temperature for 30 minutes. Ten minutes before the incubation ended, the detection antibodies were vortexed for 5 seconds and briefly centrifuged to collect the liquid. The detection antibody was diluted to 1 \times by combining 300 μL of the 10 \times detection antibody with 2700 μL of 10 \times detection antibody diluent, resulting in a total volume of 3000 μL . Following the initial incubation, the plate was subjected to three wash cycles with 100 μL of wash buffer. The diluted (1 \times) detection antibodies were gently vortexed, and 25 μL was aliquoted into each well. The plate was covered with sealing tape and incubated again at 850 ± 50 rpm at room temperature for 30 minutes. In the final 10 minutes of incubation, 100 \times streptavidin-phycoerythrin (SA-PE) was vortexed for 5 seconds and briefly centrifuged to ensure the liquid was collected. The SA-PE was diluted to 1 \times by mixing 60 μL of 100 \times SA-PE with 5940 μL of assay buffer, yielding a total volume of 6000 μL . After the incubation with detection antibodies, 100 μL of wash buffer was used to wash the plate three times. The diluted (1 \times) SA-PE was vortexed, and 50 μL was added to each well. The plate was incubated at 850 ± 50 rpm for 10 minutes at room temperature. Following the SA-PE incubation, the plate was washed three times with 100 μL of wash buffer. The beads were resuspended in 125 μL of assay buffer and shaken at 850 ± 50 rpm for 30 seconds. The sealing tape was removed, and the plate was read using the following settings: RP1 (PMT) low, DD Gates 5000 (low); 25000 (high); and Bead Events at 50.

2.2.11 DATA ANALYSIS

The experimental quantification data were analysed using the comparative threshold cycle ($\Delta\Delta\text{Ct}$) method to calculate the fold change in gene expression. The data were imported into Microsoft Excel, where Ct values for each replicate were calculated using the standard formula. These Ct values were then used to compute the fold changes, which were determined using the equation $2^{-\Delta\Delta\text{Ct}}$. Average fold changes were reported as means and standard deviations relative to the untreated control, which was normalized to 1. A One-Way ANOVA test was conducted using GraphPad Prism Version 8 (GraphPad Software, USA) to assess any significant differences between the treated samples and the control, with the significance level set at $p \leq 0.05$.

2.12 ETHICAL STATEMENT

The research proposal for this study was submitted the Health and Wellness Sciences Research Ethics Committee (HWS-REC) at Cape Peninsula University of Technology for ethical approval (CPUT/HWS-REC (2021/H24)), which was granted.

CHAPTER THREE

RESULTS

3.1 SOD AND CAT GENE EXPRESSION

Superoxide dismutase (SOD) serves to safeguard cells from damage inflicted by reactive oxygen species, particularly superoxide radicals (Abati, 2020). Conversely, the catalase (CAT) gene plays a crucial role in mitigating oxidative stress by catalysing the decomposition of hydrogen peroxide into water and oxygen, thereby reducing its harmful effects (Tehrani, 2018). All 48-hour treatments significantly reduced SOD expression levels compared to control cells ($p < 0.0001$; Figure 8A). At 72 hours, glucose alone ($p < 0.001$; Figure 8B) and both combination treatments (LCBD+G and HCBD+G) significantly decreased SOD expression ($p < 0.01$ and $p < 0.001$, respectively; Figure 8B), while low and high CBD treatments showed no significant change. All 48-hour treatments significantly increased CAT expression levels compared to control cells. Glucose treatment alone caused the highest increase in CAT expression ($p < 0.0001$; Figure 8C), while both low and high CBD treatments significantly increased CAT expression ($p < 0.001$ and $p < 0.01$, respectively; Figure 8C). Combination treatments (LCBD+G and HCBD+G) upregulated CAT expression in a similar manner to that of glucose alone ($p < 0.0001$; Figure 8C). At 72 hours, glucose alone caused a significant downregulation in CAT expression ($p < 0.05$; Figure 8D); however, the high CBD treatment upregulated CAT expression ($p < 0.05$; Figure 8D). The One-Way ANOVA test showed that the effects of glucose and high CBD were significant.

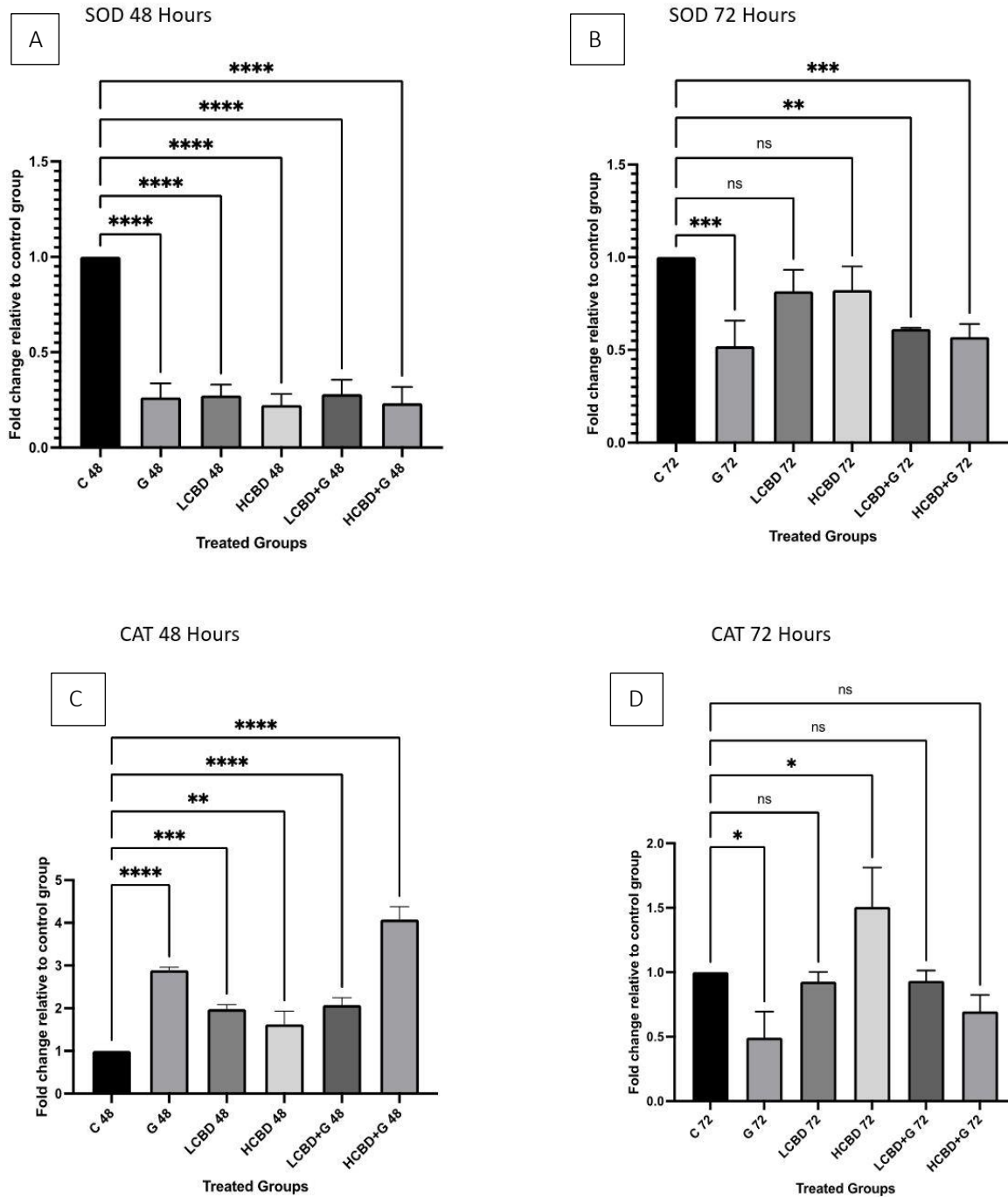


Figure 3.1. Expression of superoxide dismutase (SOD; A and B) and catalase (CAT; C and D) in HepG2 cells treated with high glucose (40 mM) and CBD (1 μ M and 5 μ M) over 48 and 72 hours. The mRNA expression was quantified using qPCR. *GAPDH* was used as the housekeeping gene. * $p < 0.05$, ** $p < 0.01$, *** $p < 0.001$, and **** $p < 0.0001$ indicate levels of significance. C, Control; G, glucose; LCBD, low CBD; HCBD, high CBD; LCBD+G, low CBD with glucose; HCBD+G, high CBD with glucose.

3.2 GPX AND NRF2 GENE EXPRESSION

Glutathione peroxidase (*GPX*) is an antioxidant enzyme that catalyses the reduction of various organic and inorganic hydroperoxides to their respective alcohols, using glutathione and other reducing agents, thereby, playing a critical role in safeguarding cells against oxidative damage (Margis, 2020). *NRF2* functions as a xenobiotic-activated receptor (XAR) that modulates the cellular adaptive response to oxidative stress and electrophilic agents (Ma, 2013). All 48-hour treatments significantly reduced *GPX* expression levels compared to control cells, except for glucose, which showed no significant changes. Both low and high CBD treatments alone reduced *GPX* expression ($p < 0.001$ and $p < 0.05$, respectively; Figure 9A). Combination treatments (LCBD+G and HCBd+G) significantly decreased *GPX* expression ($p < 0.0001$; Figure 9A). At 72 hours, combination treatment with low CBD and glucose upregulated *GPX* expression ($p < 0.0001$; Figure 9B), whereas high CBD combined with glucose caused a significant downregulation ($p < 0.05$; Figure 9B). All 48-hour treatments significantly reduced *NRF2* expression levels compared to control cells ($p < 0.0001$; Figure 9C). Glucose treatment downregulated *NRF2* expression. Both low and high CBD treatments decreased *NRF2* expression. After 72 hours, glucose treatment alone significantly downregulated *NRF2* expression ($p < 0.001$; Figure 9D). Low CBD treatment reduced *NRF2* expression, to a lower degree than glucose alone ($p < 0.05$; Figure 9D). High CBD treatment, however, upregulated *NRF2* expression ($p < 0.001$; Figure 9D). Combination treatment with low CBD and glucose resulted in a downregulation of *NRF2* expression, but less severe than with glucose alone ($p < 0.01$; Figure 9D). High CBD combined with glucose caused a downregulation similar to glucose alone ($p < 0.0001$; Figure 9D). The results from all antioxidant genes suggest that CBD provides oxidative protection to cells exposed to glucose, thereby normalizing the antioxidant response compared to glucose exposure alone.

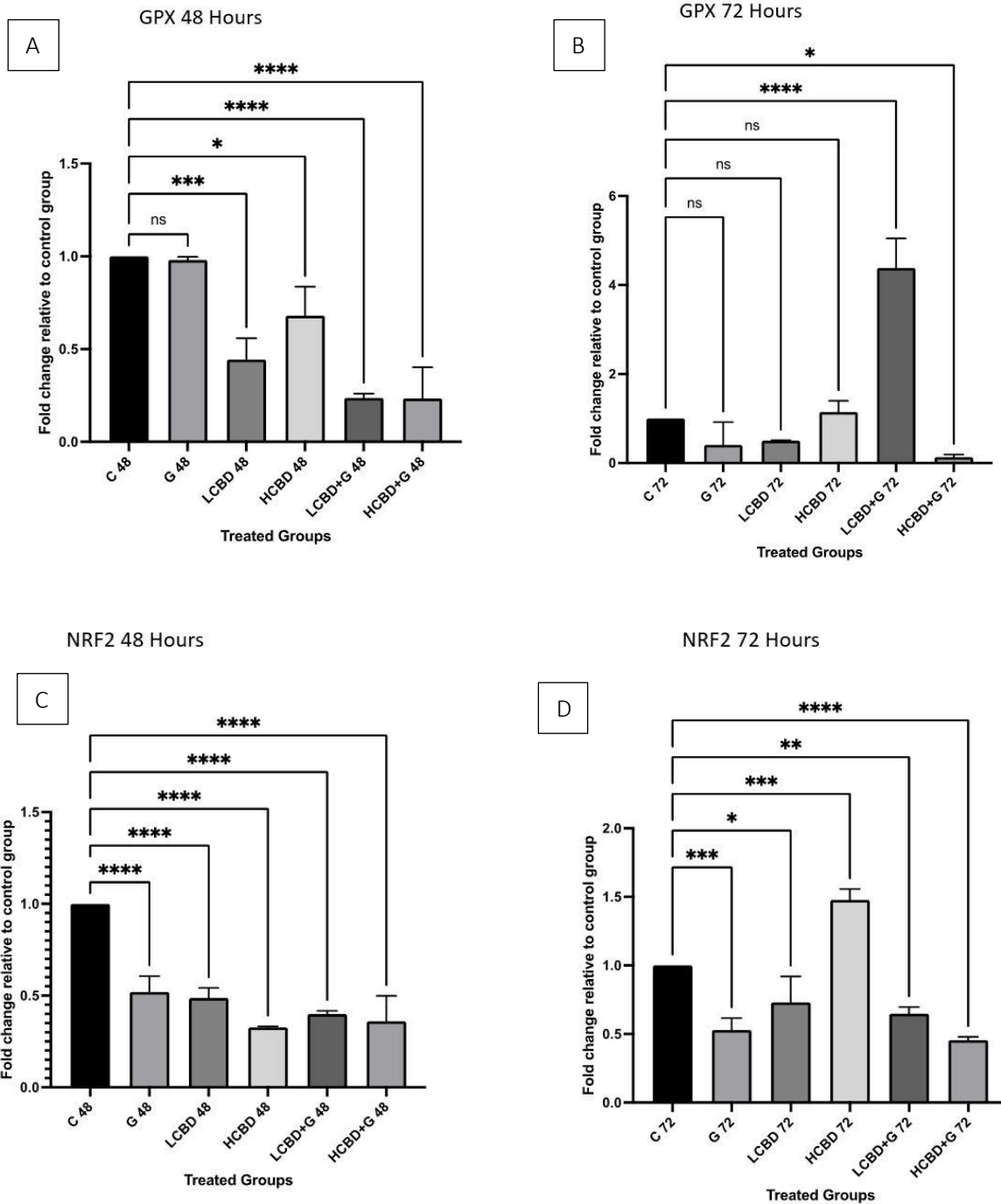


Figure 3.2. Expression of glutathione peroxidase (GPX; A and B) and nuclear factor erythroid 2-related factor 2 (NRF2; C and D) in HepG2 cells treated with high glucose (40 mM) and CBD (1 μ M and 5 μ M) over 48 and 72 hours. The mRNA expression was quantified using qPCR. *GAPDH* was used as the housekeeping gene. * $p < 0.05$, ** $p < 0.01$, *** $p < 0.001$, and **** $p < 0.0001$ indicate levels of significance. C, Control; G, glucose; LCBD, low CBD; HCBD, high CBD; LCBD+G, low CBD with glucose; HCBD+G, high CBD with glucose.

3.3 PPARG AND HIF1A GENE EXPRESSION

Activation of *PPARG* can enhance the expression of antioxidant enzymes, including *SOD*, *CAT*, and *GPX*, which collectively mitigate oxidative damage by neutralizing reactive oxygen species (ROS) (Kim, 2013). Additionally, *HIF-1 α* elevates the expression levels of *PDK1*, thereby promoting mitochondria-independent metabolic pathways. *HIF-1 α* also improves electron transfer efficiency by substituting the complex IV subunit, which reduces ROS production through the inhibition of complex IV (Bae, 2024). *HIF-1 α* is a crucial transcription factor that facilitates cellular adaptation to low oxygen levels. Its regulation is intricately influenced by both hypoxic conditions and hyperglycaemia, which play pivotal roles in the development of chronic complications associated with diabetes (Xiao, 2013). All 48-hour treatments significantly reduced *PPARG* expression levels compared to control cells. Glucose treatment alone caused a slight downregulation of *PPARG* expression ($p < 0.0001$; Figure 10A). Low and high CBD treatments resulted in a more significant downregulation of *PPARG* compared to glucose ($p < 0.0001$; Figure 10A). Combination treatments (LCBD+G and HCBD+G) also downregulated *PPARG* expression ($p < 0.001$ and $p < 0.0001$, respectively; Figure 10A).

At 72 hours, glucose treatment alone led to a significant upregulation of *PPARG* expression ($p < 0.0001$; Figure 10B). Combination treatments increased *PPARG* expression, but this increase was still lower than that seen with glucose alone ($p < 0.01$; Figure 10B). All 48-hour treatments significantly reduced *HIF1A* expression levels compared to control cells ($p < 0.0001$; Figure 10C). Glucose treatment alone, as well as low and high CBD treatments significantly decreased *HIF1A* expression ($p < 0.0001$; Figure 10C). Combination treatments with low and high CBD and glucose significantly downregulated *HIF1A* expression, comparable to the effects of glucose and CBD alone. Glucose significantly decreased *HIF1A* expression after 72 hours ($p < 0.0001$; Figure 10D), while low CBD increased *HIF1A* expression ($p < 0.05$; Figure 10D). Combination treatment with low CBD and glucose decreased *HIF1A* expression, though the expression level was still higher than that in cells treated with glucose alone ($p < 0.0001$; Figure 10D). High CBD combined with glucose caused a significant decrease in *HIF1A* expression, even lower than that observed with glucose alone ($p < 0.0001$; Figure 10D).

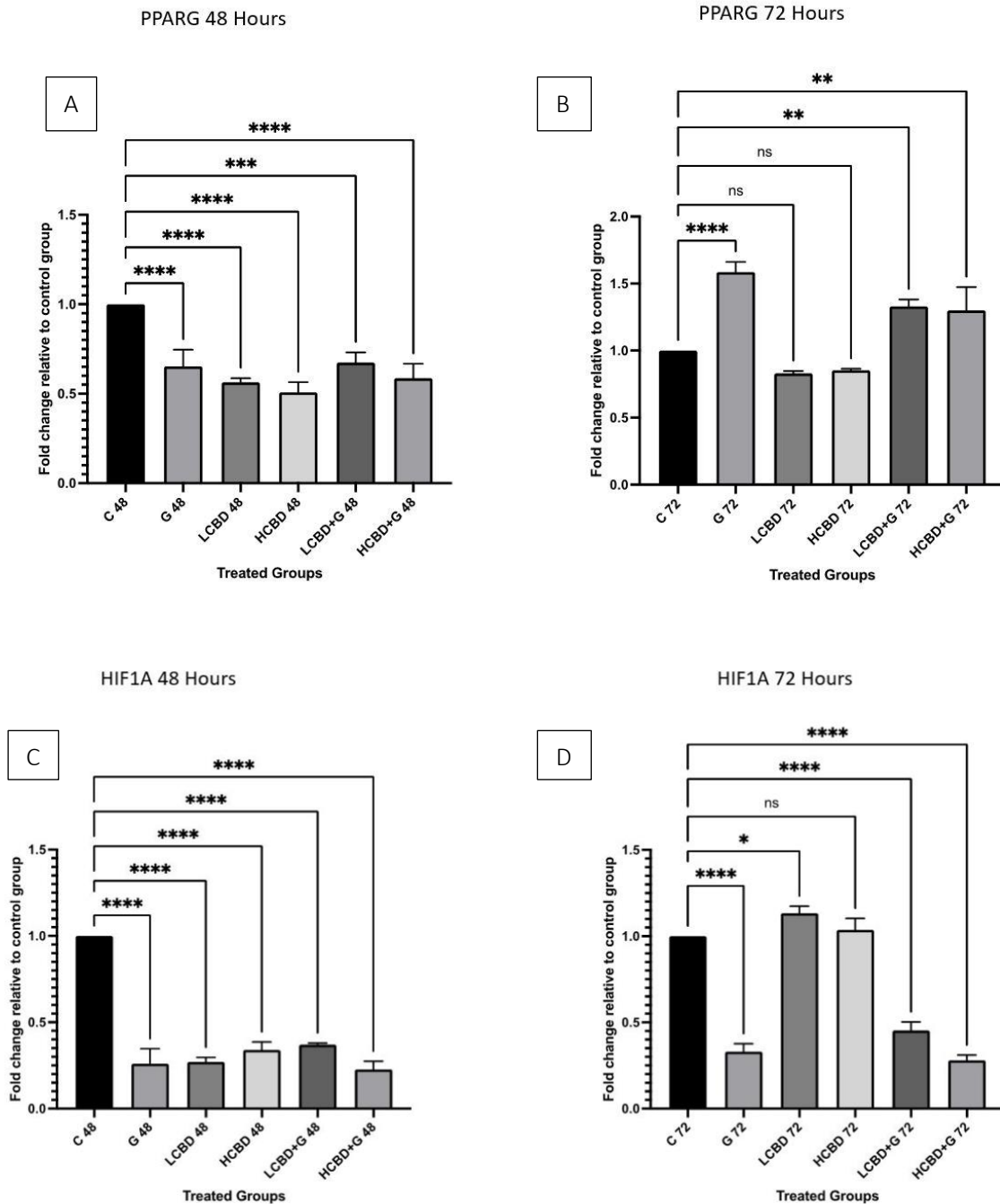


Figure 3.3. Expression of peroxisome proliferator activated receptor gamma (*PPARG*; A and B) and hypoxia-inducible factor 1alpha (*HIF1A*; C and D) in HepG2 cells treated with high glucose (40 mM) and CBD (1 μ M and 5 μ M) over 48 and 72 hours. The mRNA expression was quantified using qPCR. *GAPDH* was used as the housekeeping gene. * $p < 0.05$, ** $p < 0.01$, *** $p < 0.001$, and **** $p < 0.0001$. C, Control; G, glucose; LCBD, low CBD; HCBD, high CBD; LCBD+G, low CBD with glucose; HCBD+G, high CBD with glucose.

3.4 *NF-κB* GENE EXPRESSION

NF-κB is a transcription factor that serves as a critical regulator for activating specific immune and inflammatory pathways. *NF-κB* influences cellular behaviour by inhibiting apoptosis, promoting cell proliferation, and enhancing immune and inflammatory responses (Serasanambati, 2016). *NF-κB* may exert a protective effect during oxidative stress by inhibiting the accumulation of reactive oxygen species (ROS). Inhibition of *NF-κB* activation results in elevated ROS production triggered by *TNFα*, along with increased lipid peroxidation and protein oxidation (Lingappan, 2018). All 48-hour treatments, except glucose, significantly impacted *NF-κB* expression levels compared to control cells. Both low and high doses of CBD increased *NF-κB* expression ($p < 0.0001$ and $p < 0.05$, respectively; Figure 11A); however, when combined with glucose, both low and high doses of CBD reduced *NF-κB* expression to levels similar to those seen with glucose alone ($p < 0.05$ and $p < 0.001$; respectively; Figure 11A). After 72 hours, glucose treatment alone caused a significant reduction in *NF-κB* expression ($p < 0.001$; Figure 11B). Low CBD led to an increase in *NF-κB* expression ($p < 0.05$; Figure 11B). Combination treatments with low and high CBD and glucose resulted in a decrease in *NF-κB* expression ($p < 0.001$ and $p < 0.05$, respectively; Figure 11B). These findings imply that CBD may trigger an immune response that reverses the low-grade inflammation caused by a high glucose environment.

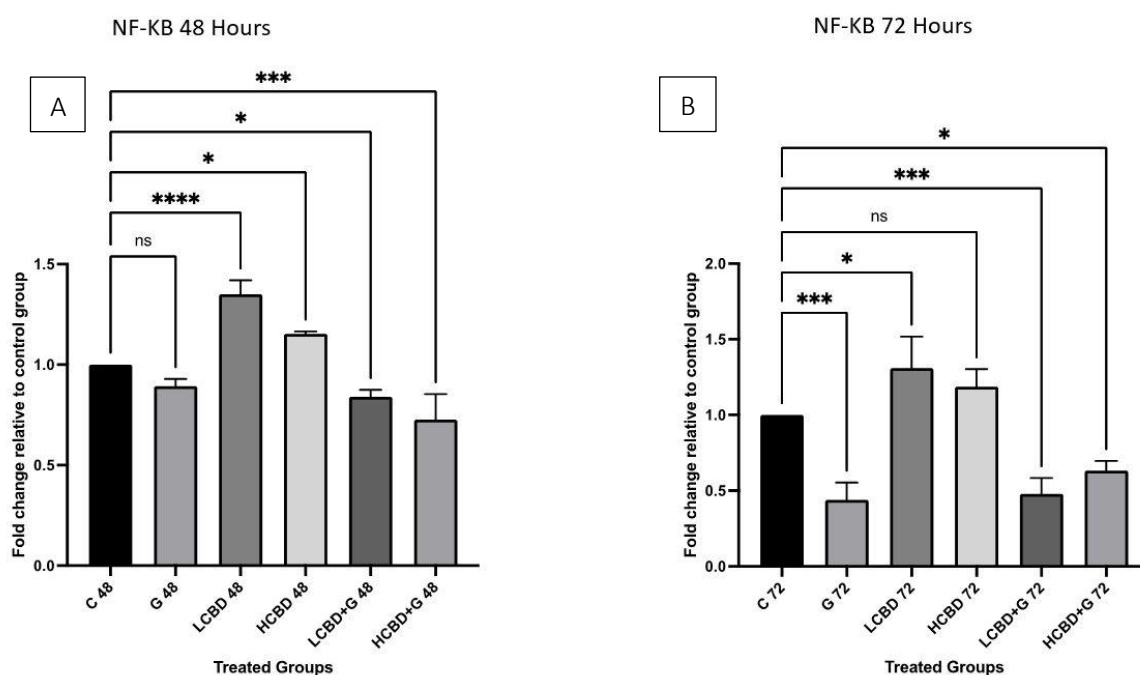


Figure 3.4. Expression of nuclear factor kappa-light-chain-enhancer of activated B cells (*NF-κB*) in HepG2 cells treated with high glucose (40 mM) and CBD (1 μM and 5 μM) over 48 hours (A) and 72 hours (B). The mRNA expression was quantified using qPCR. *GAPDH* was used as the housekeeping gene. * $p < 0.05$, ** $p < 0.01$, *** $p < 0.001$, and **** $p < 0.0001$. C, Control; G, glucose; LCBD, low CBD; HCBD, high CBD; LCBD+G, low CBD with glucose; HCBD+G, high CBD with glucose.

3.5 MIRNA 34A GENE EXPRESSION

All 48-hour treatments, except high CBD with glucose, significantly impacted miRNA-34a expression levels compared to control cells. Glucose ($p < 0.0001$; Figure 12A), low CBD ($p < 0.001$; Figure 12A), and both combination groups (LCBD+G and HCBD+G) increased the expression of miRNA-34a ($p < 0.0001$; Figure 12A). Only high CBD decreased miRNA-34a expression ($p < 0.0001$; Figure 12A). Interestingly, after 72 hours, glucose ($p < 0.0001$; Figure 12B) and both combination groups (LCBD+G and HCBD+G) significantly downregulated miRNA-34a expression ($p < 0.0001$; Figure 12B). Low CBD ($p < 0.001$; Figure 12B) and high CBD ($p < 0.05$; Figure 12B) treatments greatly increased miRNA-34a expression. These results indicate that glucose downregulates miRNA-34a expression, while CBD upregulates miRNA-34a, suggesting that CBD may regulate miRNA expression disrupted by high levels of glucose.

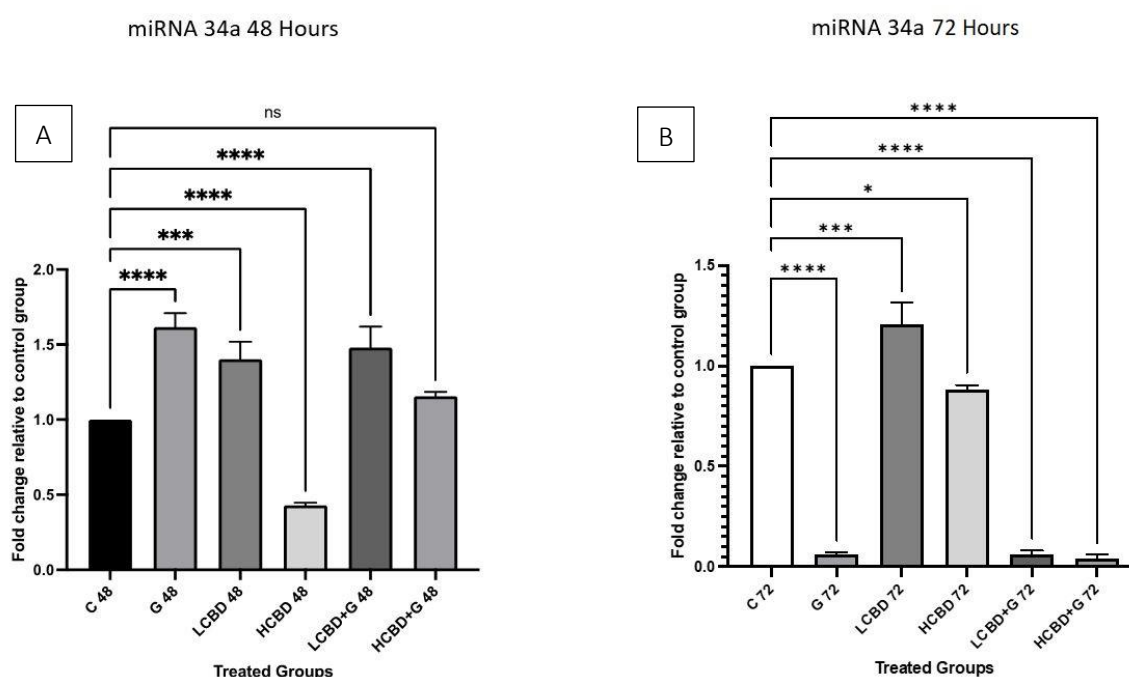


Figure 3.5. Expression of miRNA-34a in HepG2 cells treated with high glucose (40 mM) and CBD (1 μ M and 5 μ M) over 48 hours (A) and 72 hours (B). The miRNA expression was quantified using qPCR. U6 SnRNA (V2) was used as the housekeeping gene. * $p < 0.05$, ** $p < 0.01$, *** $p < 0.001$ and **** $p < 0.0001$. C, Control; G, glucose; LCBD, low CBD; HCBD, high CBD; LCBD+G, low CBD with glucose; HCBD+G, high CBD with glucose.

3.6 IL-6 CYTOKINE CONCENTRATIONS

Interleukin-6 (IL-6) mitigates oxidative stress by promoting autophagy and enhancing the accumulation of *NRF2*, a central regulator of the antioxidant response (Marasco, 2018). Additionally, IL-6 drives inflammatory responses by initiating the transcription of various factors involved in multiple inflammatory pathways (Rose-John, 2018). At 48 hours, glucose significantly decreased the concentration of IL-6 cytokine ($p < 0.0001$; Figure 13A). Treatment with low concentrations of CBD resulted in an even greater reduction than glucose alone ($p < 0.0001$; Figure 13A). High concentrations of CBD also reduced the cytokine concentration

compared to the control, although this reduction was less pronounced than that observed with glucose treatment ($p < 0.01$; Figure 13A). Both combination treatments resulted in a more substantial decrease in cytokine concentration than glucose alone ($p < 0.0001$; Figure 13A). At 72 hours, glucose eliminated IL-6 to undetectable levels ($p < 0.0001$; Figure 13B). Although both concentrations of CBD and the combination treatments reduced cytokine levels relative to the control, these reductions were markedly reduced compared to those achieved by glucose ($p < 0.0001$; Figure 13B). The results indicate that CBD may restore and correct the IL-6 levels that were significantly reduced in high glucose environment.

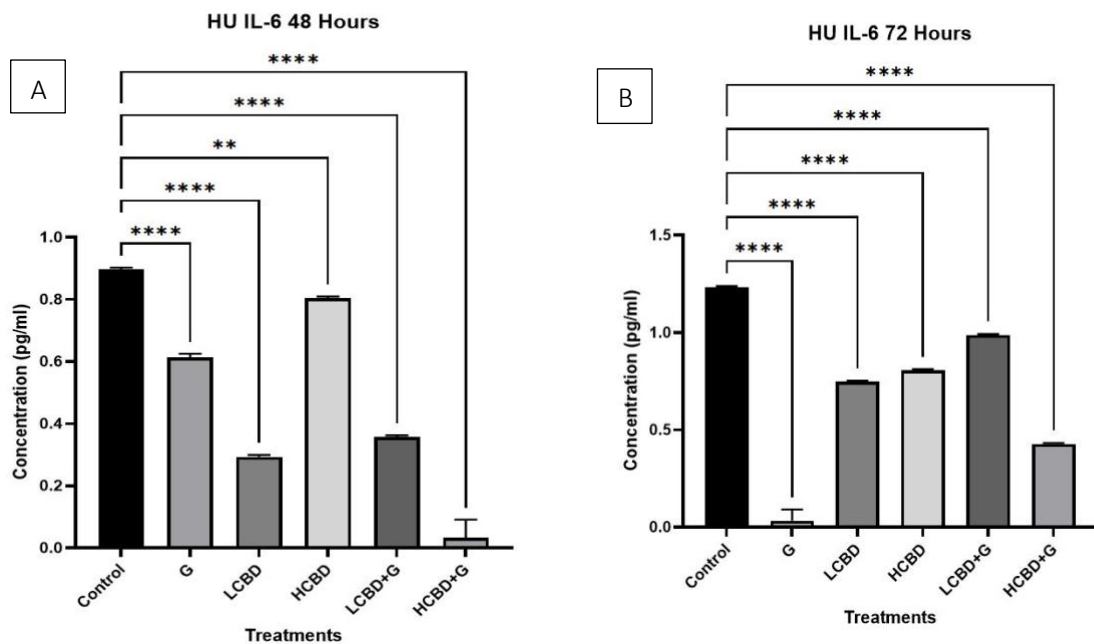


Figure 3.6. Concentrations of HU-IL-6 cytokine in HepG2 cells treated with high glucose (40 mM) and CBD (1 μ M and 5 μ M) over 48 (A) and 72 hours (B). * $p < 0.05$, ** $p < 0.01$, *** $p < 0.001$, and **** $p < 0.0001$. C, Control; G, glucose; LCBD, low CBD; HCBD, high CBD; LCBD+G, low CBD with glucose; HCBD+G, high CBD with glucose.

3.7 IL-8 CYTOKINE CONCENTRATIONS

Interleukin-8 (IL-8) is a chemotactic cytokine produced by various blood cells and tissues. Unlike other cytokines, IL-8 shows a particular affinity for neutrophils, with limited effects on other blood cell types (Bickel, 1993). IL-8 plays a crucial role in inflammatory responses by recruiting and activating neutrophils at sites of inflammation (Bickel, 1993). All treatments significantly affected IL-8 cytokine levels at 48 hours. Both glucose, low CBD and the combination of low CBD with glucose resulted in a comparable and significant increase in cytokine concentration ($p < 0.0001$; Figure 14A). While treatments with high CBD, and high CBD with glucose also led to a decrease in concentration, these effects were less pronounced than those observed with glucose alone or low CBD combined with glucose ($p < 0.0001$; Figure 14A). At 72 hours, the concentrations observed with glucose and low CBD were similar to those of the control ($p < 0.0001$; Figure 14B). High CBD was the only treatment that significantly

reduced IL-8 cytokine concentration ($p < 0.0001$; Figure 14B). Conversely, both combination treatments significantly increased IL-8 levels ($p < 0.0001$; Figure 14B). These findings suggest that CBD may modulate and mitigate the immune response triggered by exposure to high glucose levels.

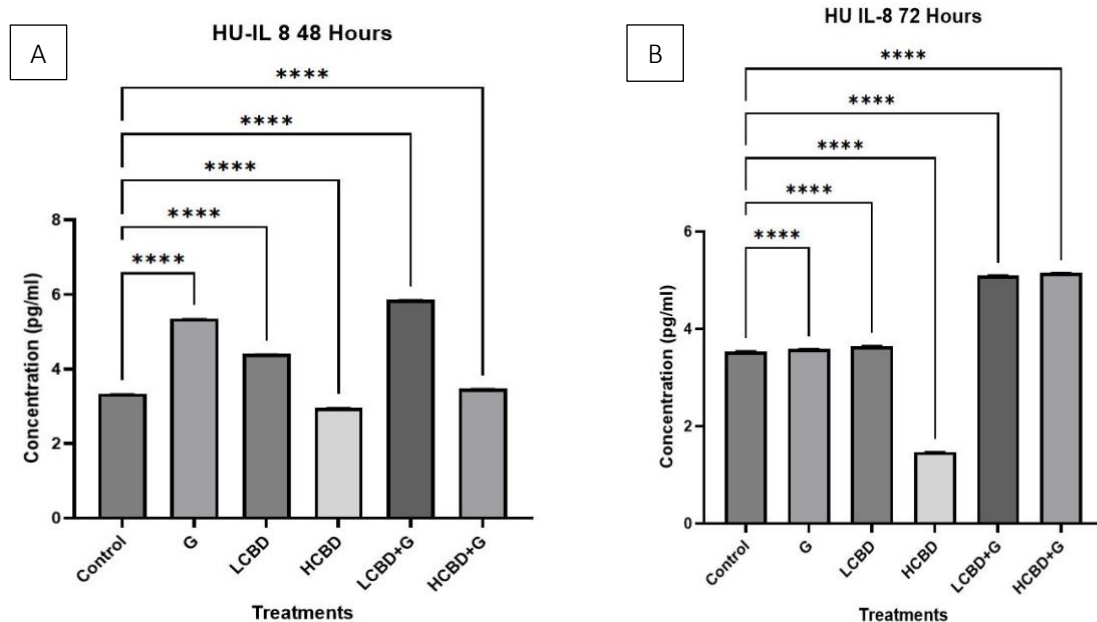


Figure 3.7. Concentrations of HU-IL-8 cytokine in HepG2 cells treated with high glucose (40 mM) and CBD (1 μ M and 5 μ M) over 48 (A) and 72 hours (B). * $p < 0.05$, ** $p < 0.01$, *** $p < 0.001$, and **** $p < 0.0001$. C, Control; G, glucose; LCBD, low CBD; HCBD, high CBD; LCBD+G, low CBD with glucose; HCBD+G, high CBD with glucose.

3.8 IL-9 CYTOKINE CONCENTRATIONS

Beyond its pro-inflammatory effects, interleukin-9 (IL-9) has demonstrated anti-inflammatory properties, contingent on the cell types expressing it and the microenvironment in which it is produced. The secretion of IL-9 by regulatory T cells (Tregs) contributes to immune tolerance (Ayakannu, 2019). At 48 hours, glucose and both combination treatments markedly reduced the concentration of IL-9 to nearly undetectable levels ($p < 0.0001$; Figure 15A). In contrast, treatment with both concentrations of CBD alone resulted in a significant increase in IL-9 levels ($p < 0.0001$; Figure 15A). At 72 hours, glucose and high CBD in combination with glucose significantly reduced IL-9 levels to near zero ($p < 0.0001$; Figure 15B). Meanwhile, low-concentration CBD caused a slight reduction, whereas high-concentration CBD led to a slight increase in IL-9 levels ($p < 0.0001$; Figure 15B). Notably, the combination of low-concentration CBD with glucose significantly elevated IL-9 levels compared to the control ($p < 0.0001$; Figure 15B). These results suggest that CBD may counteract the inflammatory response induced by high glucose conditions.

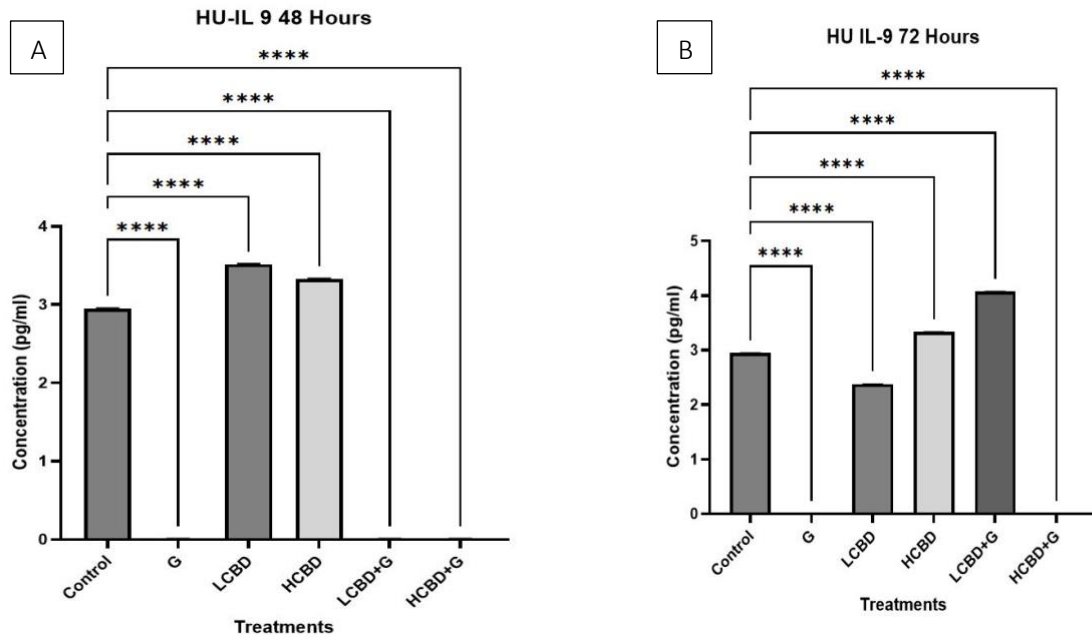


Figure 3.8. Concentrations of HU-IL-9 cytokine in HepG2 cells treated with high glucose (40 mM) and CBD (1 μ M and 5 μ M) over 48 (A) and 72 hours (B). * $p < 0.05$, ** $p < 0.01$, *** $p < 0.001$, and **** $p < 0.0001$. C, Control; G, glucose; LCBD, low CBD; HCBD, high CBD; LCBD+G, low CBD with glucose; HCBD+G, high CBD with glucose.

3.9 PDGF-BB CYTOKINE CONCENTRATIONS

Platelet-derived growth factor-BB (PDGF-BB) is crucial in regulating inflammation by suppressing the production of chemokines and pro-inflammatory cytokines (Krzystek-Korpicka, 2009). As one of the most prevalent growth factors found in platelet-derived products, PDGF-BB has been demonstrated to promote tissue regeneration following injury (Mihaylova, 2018). After 48 hours, low CBD, low CBD with glucose, and high CBD with glucose all significantly reduced the concentration of PDGF-BB to undetectable levels ($p < 0.0001$; Figure 16A). Although high CBD also reduced PDGF-BB concentration, the decrease was only slight compared to the control ($p < 0.0001$; Figure 16A). At 72 hours, all treatments resulted in a significant increase in PDGF-BB concentration, as the control level was zero. The increases observed with low CBD and high CBD in combination with glucose were less pronounced than those with glucose alone ($p < 0.0001$; Figure 16B). Conversely, high CBD and low CBD with glucose both exhibited a greater increase in PDGF-BB levels compared to glucose alone ($p < 0.0001$; Figure 16B). These results suggest that CBD may facilitate the repair of tissue damage induced by a high-glucose environment.

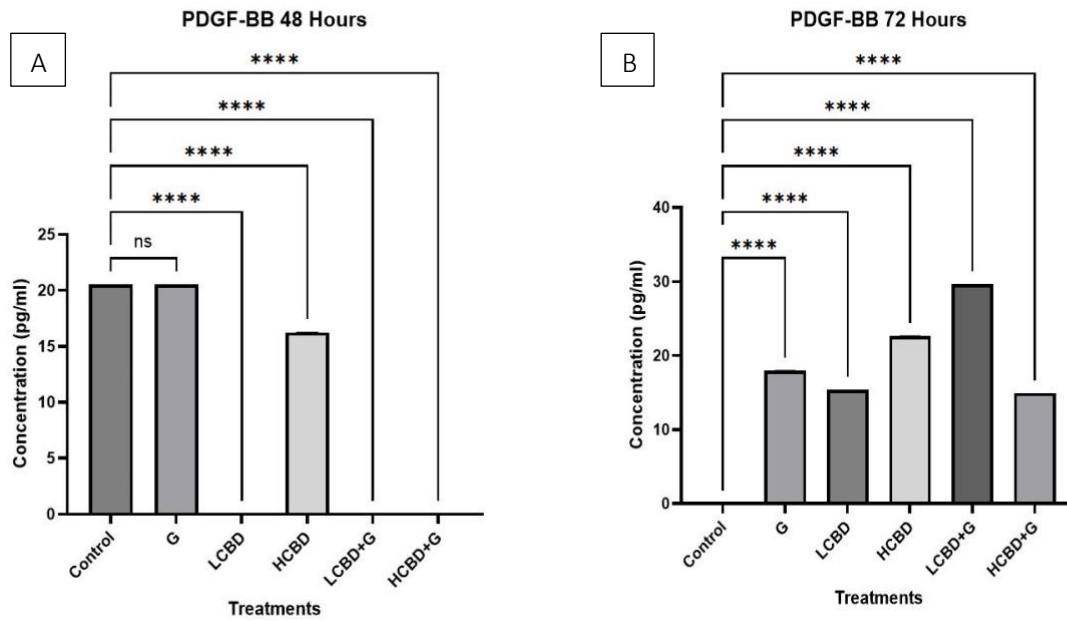


Figure 3.9. Concentrations of PDGF-BB cytokine in HepG2 cells treated with high glucose (40 mM) and CBD (1 μ M and 5 μ M) over 48 (A) and 72 hours (B). * $p < 0.05$, ** $p < 0.01$, *** $p < 0.001$, and **** $p < 0.0001$. C, Control; G, glucose; LCBD, low CBD; HCBD, high CBD; LCBD+G, low CBD with glucose; HCBD+G, high CBD with glucose.

CHAPTER FOUR

DISCUSSION

Oxidative stress induced by elevated glucose levels has been demonstrated to play a key role in the initiation and progression of diabetes. The activation of the immune system is closely linked to the incidence and progression of type 2 diabetes, with both adaptive and innate immune responses playing significant roles in tissue inflammation (Tsalamandris, 2019). The South African healthcare system is increasingly burdened with cases of non-communicable diseases. Thus, it is essential to identify innovative methods to treat or prevent DM and related illnesses. CBD is reportedly a potent antioxidant, which protects cells against chemical damage due to oxidation, and could contribute to protecting against the development of diabetes and certain types of cancer (Farhat, 2011). In this study, we examined the expression of genes related to oxidative stress, glucose metabolism, and inflammation in HepG2 cells exposed to elevated glucose levels, while evaluating the impact of CBD on these gene expressions.

Normal cellular metabolism produces biological free radicals, which are highly unstable molecules. At high levels, free radicals cause damage to cell structures, and at low levels free radicals act as a defence against infectious agents and aid in the maturation process of cellular structures (Oguntibeju, 2019). In this study, we measured the mRNA expression of *CAT*, *SOD*, *GPx-1*, and *Nrf2* genes. Superoxide dismutase (SOD) is the initial detoxifying enzyme and the most potent antioxidant within the cell. This crucial endogenous antioxidant plays a pivotal role as part of the primary defence system against ROS. It facilitates the conversion of two molecules of superoxide anion (*O_2) into hydrogen peroxide (H_2O_2) and molecular oxygen (O_2) through a process called dismutation. This effectively reduces the potential harm posed by superoxide anions (Ighodaro, 2018). *GPx-1* is responsible for preventing the harmful build-up of hydrogen peroxide within cells and can reduce lipid hydroperoxides and other soluble hydroperoxides once they are released from membrane lipids (Lubos, 2011). Nuclear factor erythroid 2-related factor 2 (*Nrf2*) serves as the key regulator in the cellular transcriptional response to oxidative stress. *Nrf2* oversees the activation of various genes responsible for antioxidants and phase II enzymes (Ngo, 2022). Catalase (*CAT*) is an important antioxidant enzyme, present in most aerobic organisms, that plays a crucial role in breaking down two molecules of hydrogen peroxide into one molecule of oxygen and two molecules of water through a two-step reaction (Nandi, 2019). It is important to study these genes as they all play an important role in the antioxidant response of the cell.

Our results show a significant downregulation in the expression of *CAT*, *SOD*, *GPx-1*, and *Nrf2* genes in HepG2 cells after exposure to high glucose concentrations for 48 and 72 hours. These results agree with previous studies (Wang and Guo, 2019; Subramaniyan, 2017; Ahmadvand, 2023). In a study by Ahmadvand, both *CAT* and *GPX* genes were downregulated in HepG2 cells when exposed to glucose, even though a higher concentration of 60 mM of glucose was used. These results suggest a weakness in the cellular defence against oxidative damage triggered by high glucose levels, which may reduce the activity of antioxidant enzymes.

In this study, we also measured the mRNA expression of *PPARG*, *HIF-1 α* , and *NF- κ B* genes. *PPARG* has a negative effect on insulin signalling and is activated by oxidative stress (Rain,

2011). The relationship between glucose and *HIF-1 α* is, in some cases, bidirectional. *HIF-1 α* has been shown to regulate the expression of nearly all enzymes involved in glycolysis, as well as GLUT1 and GLUT3, which are responsible for cellular glucose uptake. Conversely, glucose levels, along with glucose uptake and glycolysis, affect the stability and activation of *HIF-1 α* (Xiao, 2013). *HIF-1 α* in response to oxidative stress, orchestrates adaptive reactions by relocating to the cell nucleus and controlling gene expression. Alterations in mitochondria play a crucial role in this adaptive reaction to oxidative stress (Li, 2019). *NF- κ B* may have a protective function during oxidative stress by reducing the build-up of ROS. When *NF- κ B* activation is inhibited, there is a rise in *TNF α* -induced ROS production, along with increased lipid peroxidation and protein oxidation (Lingappan, 2018). Chronic low-grade inflammation has been identified as an independent predictor of all-cause mortality in high-risk individuals with type 2 diabetes, though it does not significantly predict cardiovascular events. Targeting chronic low-grade inflammation could represent a therapeutic approach to reduce residual cardiovascular risk in patients with type 2 diabetes (Sharif, 2021).

Previous literature suggests that high glucose environments downregulate *PPARG* gene expression (Way, 2001; Patel, 2009; Indira, 2013). *PPARG* gene expression levels at 48 hours align with previous literature. Our findings for *HIF-1 α* align with previous literature that states that *HIF-1 α* will be downregulated in a high glucose environment (Gunton, 2020; Garcia-Pastor, 2019). In our study, *NF- κ B* gene expression was downregulated in the high-glucose environment, which contrasts with previous literature suggesting that *NF- κ B* should be upregulated under similar conditions. High glucose may disrupt signalling pathways upstream of *NF- κ B* by impairing the activity of protein kinases and inhibitors essential for its activation. Furthermore, glucose-induced metabolic changes could alter chromatin structure and transcriptional machinery, potentially reducing *NF- κ B* transcriptional activity. These mechanisms were not investigated in this study, and further research is required to elucidate the cause of *NF- κ B* downregulation in a high-glucose environment (Panahi, 2018; Alnahdi, 2019).

The 48-hour exposure of HepG2 cells to the treatments may be insufficient to fully observe the effects of CBD on gene expression. However, at 72 hours, CBD upregulated *SOD* compared to the glucose treatment group. Both the low and high concentrations of CBD reversed the upregulating effects of glucose on the *CAT* gene. This suggests that while glucose induces upregulation of *CAT* by promoting oxidative stress in the cell, CBD may exert an opposing effect. The *GPx-1* gene responded to the low concentration of CBD only. As CBD research is still in its early stages, further investigation is required to determine the optimal dose of CBD. The *Nrf2* gene exhibited a more pronounced response to a low concentration of CBD compared to a higher concentration. These results show that CBD may oppose glucose-induced downregulation of antioxidant genes. Previous literature has shown that CBD upregulated antioxidant genes, although most research was conducted in other cell types or in mouse models; nevertheless, the results show that CBD exhibits antioxidant properties (Atalay, 2019; Khaksae, 2022; Campos, 2017; Garcia-Arencibia, 2007).

Our results suggest that a 48-hour exposure period is inadequate to elicit significant alterations in gene expression following CBD treatment. However, after 72 hours, CBD was found to downregulate the expression of the *PPARG* gene in comparison to glucose alone, suggesting that CBD may counteract the effects of glucose in HepG2 cells. Although glucose

downregulated *HIF-1 α* expression, a low concentration of CBD was observed to upregulate this gene, further suggesting a potential antagonistic effect of CBD against glucose. Reduced expression of *HIF-1 α* is associated with poor glycaemic control, while the upregulation of this gene by CBD suggests that CBD may enhance diabetes management outcomes (Ziello, 2007). Similarly, while glucose downregulated *NF- κ B* expression, a high concentration of CBD resulted in a slight upregulation. These findings imply that CBD may reverse some of the effects of glucose, though further research is required to confirm these results and elucidate the underlying mechanisms.

MicroRNAs (miRNA) have become more important in diagnosis and detecting diseases in the human body. MicroRNAs are small non-coding RNAs that serve a vital function in the regulation of gene expression (Rong, 2013). miR-34a contributes to endothelial dysfunction and vascular aging in diabetes, which heightens the overall risk of oxidative stress and inflammation (Mone, 2022). In this study, the expression of miRNA-34a was upregulated by exposure to CBD. This is consistent with previous literature, which reported that miR-34a expression was upregulated in BV-2 microglial cells exposed to 10 μ M CBD. Although a different cell line and CBD concentration were utilized in that study, the upregulation of miR-34a by CBD was still observed (Juknat, 2019).

Our findings suggest that at 48 hours, glucose increased the expression of miRNA-34a, while a high concentration of CBD reduced its expression. In the combination treatments, both low and high concentrations of CBD decreased miRNA-34a expression compared to glucose alone. At 72 hours, glucose downregulated miRNA-34a expression, whereas a low concentration of CBD increased it. The combination treatments produced similar effects to glucose. These results suggest that CBD may enhance miRNA-34a expression, potentially mitigating the disruptive effects of glucose. Further research with extended time frames is required to validate these findings.

Researchers have observed elevated levels of inflammation in individuals diagnosed with type 2 diabetes. Specifically, the concentration of inflammatory mediators known as cytokines is frequently higher in individuals with type 2 diabetes compared to those without the condition. As type 2 diabetes progresses, the body's sensitivity to insulin diminishes, leading to insulin resistance, which subsequently contributes to increased inflammation (Hoffman, 2023). This process can establish a detrimental feedback loop, where elevated inflammation exacerbates insulin resistance and vice versa (Hoffman, 2023). In this study, we investigated the impact of CBD on inflammatory cytokines to determine its potential effects on low-grade inflammation.

Interleukin-6 (IL-6), a multifunctional cytokine, is associated with the pathophysiology of type 2 diabetes (T2D). Increased circulating levels of IL-6 act as an independent predictor of T2D and are linked to the onset of inflammation, insulin resistance, and β -cell dysfunction (Akbari, 2018). Our findings showed that glucose reduced IL-6 concentrations at 48 and 72 hours, indicating that glucose inhibits the inflammatory response. The short exposure duration may have been insufficient to replicate effects seen in other studies, as liver cells are resilient to stressors. It is possible that the glucose concentration and time frame were not sufficient to elicit stronger effects, and longer exposure may yield more pronounced results and insights into the underlying mechanisms of action. High CBD doses increased IL-6 levels, indicating a potential stimulatory effect on inflammation. Both glucose-CBD combination treatments reduced IL-6, with the high dose CBD nearly eliminating IL-6, suggesting a strong suppressive

effect. After 72 hours, glucose alone suppressed IL-6 to nearly undetectable levels, highlighting its disruptive effect on inflammatory signalling. Both low and high doses of CBD alone reduced IL-6 compared to the control, but less than glucose alone, indicating CBD may modulate the inflammatory response. The combination of low dose CBD and glucose elevated IL-6 levels compared to glucose alone, indicating that, despite glucose's suppressive effects, CBD exerts a more effective anti-inflammatory role by promoting IL-6. The high dose CBD-glucose combination also raised IL-6, though less than the low dose combination, suggesting that while the higher dose may be excessive, it still exerts an inflammatory effect. The results indicate that glucose exposure significantly suppressed both inflammatory and anti-inflammatory immune responses. Treatment with CBD, however, helped to restore a balanced cellular response to inflammation. The *NF- κ B* gene, known to activate the inflammatory pathway, was upregulated by CBD in our study. This upregulation also correlated with increased IL-6 levels, contributing to the normalization of cellular response in a high-glucose environment.

IL-8, a pro-inflammatory chemokine belonging to the CXC family, is produced by immune and other cell types in response to inflammatory stimuli. Its main function is to recruit neutrophils to areas of inflammation, while also promoting the growth and differentiation of monocytes into macrophages, enhancing endothelial cell survival and proliferation, and facilitating angiogenesis (Vilotic, 2022). At 48 hours, glucose alone increased IL-8 levels, indicating an upregulation of the immune response. Low dose CBD also elevated IL-8, though less than glucose, suggesting a modulatory effect. In contrast, high dose CBD reduced IL-8, indicating a potential anti-inflammatory effect. The combination of glucose with low dose CBD further raised IL-8, suggesting the CBD concentration was insufficient to counteract the immune response produced by glucose. However, the glucose-high CBD combination normalized IL-8 levels, indicating that an optimal CBD concentration may stabilize the immune response. At 72 hours, neither glucose nor low dose CBD significantly affected IL-8, but high dose CBD decreased IL-8, suggesting suppression of the immune response and anti-inflammatory effects. Both combination treatments increased IL-8, indicating activation of the immune response at these doses – which may occur in response to cellular stress or injury as a result of the prolonged cell culture period or the presence of high glucose levels.

A key function of IL-9 is to stimulate the growth and activity of mast cells, though its primary effects are most evident during responses to pathogenic challenges, as basal mast cell levels remain unchanged in the absence of IL-9 (Goswami, 2011). Glucose reduced IL-9 concentration to zero after exposure for 48 hours, indicating significant cellular stress. Both low and high doses of CBD increased IL-9, suggesting a protective effect. However, the glucose-CBD combinations also reduced IL-9 to zero, implying that the exposure duration may have been too short for CBD to counteract the effects of high glucose levels. At 72 hours, glucose again reduced IL-9 to zero, reinforcing its role in inducing cellular inflammation. Low dose CBD slightly decreased IL-9, suggesting a mild negative effect, while high dose CBD increased IL-9, indicating a stronger protective effect. The glucose-low CBD combination raised IL-9, suggesting that CBD may produce pro-inflammatory effects. However, the glucose-high CBD combination again reduced IL-9 to zero, hinting that high doses may overwhelm the cells, causing harm.

Platelet-derived growth factor-BB (PDGF-BB) is one of the key growth factors present in platelet-derived products and has been shown to facilitate tissue regeneration following injury

(Mihaylova, 2018). After 48 hours of exposure, glucose had no effect on PDGF-BB levels, but low dose CBD and both combination treatments completely reduced PDGF-BB, suggesting CBD may impair the cell's repair mechanisms, possibly due to the short exposure time. High dose CBD also lowered PDGF-BB but to a lesser extent, suggesting a more beneficial effect at higher concentrations. At 72 hours, high dose CBD increased PDGF-BB, suggesting support for cellular repair. The low dose CBD-glucose combination raised PDGF-BB, indicating potential repair aid in a high glucose environment, whereas the high dose combination reduced PDGF-BB, suggesting that excessive CBD may impair the cell's recovery process.

These results suggest that CBD may serve as a promising therapeutic agent or adjuvant therapy for metabolic disruptions associated with diabetes, such as dysglycaemia, low-grade inflammation, and increased oxidative stress. Further research in different *in vitro* and *in vivo* models are required to confirm the effects of CBD, elucidate the underlying mechanisms, and validate these findings.

CHAPTER FIVE

LIMITATIONS AND STRENGTHS

Further downstream analysis is required to assess protein levels, as examining gene expression alone is insufficient to determine whether CBD induces phenotypic and functional changes in cells. This study was limited to HepG2 cells; however, additional cell lines should be included, as the liver is not the only organ impacted by glucose dysregulation and metabolic dysfunction. Investigating the effects of CBD on additional cell types would provide a more comprehensive understanding of how CBD influences the human body. Furthermore, additional concentrations of both glucose and CBD should be explored. Different individuals have varying glucose levels, and studying only a high glucose concentration may not reflect the effects in those with lower glucose levels. Moreover, only two concentrations of CBD were tested, and some genes did not respond to either. Therefore, future studies should incorporate a wider range of CBD concentrations to gain clearer insights into its effects. The study was also limited to two experimental time points, both of which were relatively short. As a result, the long-term effects of CBD on gene expression remain unclear. Extending the study to include longer time frames would help in understanding the sustained impact of CBD on cellular gene expression. Additionally, *in vivo* studies using diabetic mice models, would be beneficial in revealing the effects of CBD in a holistic system and at a physiological level. There is a lack of data to indicate whether glucose does in fact induce oxidative stress and whether CBD ameliorates it. This *in vitro* study offers valuable insights into how CBD impacts HEG2 cells in a high-glucose environment. By controlling experimental conditions and minimizing variability, the study enables the focused investigation of specific gene expressions while eliminating the influence of external factors. Additional strengths include the ability to perform precise manipulations, replicate conditions consistently, and provide a cost-effective and ethical approach compared to *in vivo* studies. These factors enhance the reliability and relevance of the findings for understanding CBD's cellular effects.

Conclusion

Taken together, while CBD remains a relatively novel therapeutic compound, further investigation is necessary to fully understand its mechanisms of action. This study highlights CBD's potential in modulating oxidative stress and inflammation, which are key pathological features of diabetes mellitus. Our findings suggest that CBD influences the expression of critical genes within oxidative stress, glucose metabolism, and inflammatory pathways, as well as cytokines involved in inflammatory responses. The notable changes observed in cells treated with both CBD and glucose indicate that CBD may possess antioxidant and anti-inflammatory properties in this context. CBD efficacy seems to be limited to specific pathways and these should be the areas of focus going forward. If CBD can effectively reduce oxidative stress and inflammation, it may offer a promising natural therapeutic approach for managing diabetes-related complications and potentially contribute to more holistic diabetes management strategies.

REFERENCES

- Abati, E., Bresolin, N., Comi, G. and Corti, S., 2020. Silence superoxide dismutase 1 (SOD1): a promising therapeutic target for amyotrophic lateral sclerosis (ALS). *Expert opinion on therapeutic targets*, 24(4), pp.295-310.
- Addgene., 2020. RNA Extraction Without a Kit. Available at: <https://www.addgene.org/protocols/kit-free-rna-extraction> (Accessed: 10 April 2020)
- Adeva-Andany, M.M., Pérez-Felpete, N., Fernández-Fernández, C., Donapetry-García, C. and Pazos-García, C., 2016. Liver glucose metabolism in humans. *Bioscience reports*, 36(6).
- Ahmadvand, H., Yazdi, M., Nafari, A., Azadpour, M., Alaei, M., Moradi, F. H., Choghakhori, R., & Hormozi, M., 2023. Protective Effects of Cinnamic Acid Against Hyperglycaemia Induced Oxidative Stress and Inflammation in HepG2 Cells. In *Reports of Biochemistry & Molecular Biology* (Vol. 12, Issue 1).
- Aizpurua-Olaizola, O., Elezgarai, I., Rico-Barrio, I., Zarandona, I., Etxebarria, N. and Usobiaga, A., 2017. Targeting the endocannabinoid system: future therapeutic strategies. *Drug discovery today*, 22(1), pp.105-110.
- Akbari, M. and Hassan-Zadeh, V., 2018. IL-6 signalling pathways and the development of type 2 diabetes. *Inflammopharmacology*, 26, pp.685-698.
- Allameh, A., Niayesh-Mehr, R., Aliarab, A., Sebastiani, G. and Pantopoulos, K., 2023. Oxidative stress in liver pathophysiology and disease. *Antioxidants*, 12(9), p.1653.
- Alshaarawy, O. and Anthony, J.C., 2015. Cannabis smoking and diabetes mellitus: results from meta-analysis with eight independent replication samples. *Epidemiology (Cambridge, Mass.)*, 26(4), p.597.
- American Diabetes Association., 2016. 2. Classification and diagnosis of diabetes. *Diabetes care*, 39(Supplement 1), pp. S13-S22.
- Alnahdi, A., John, A. and Raza, H., 2019. Augmentation of glucotoxicity, oxidative stress, apoptosis and mitochondrial dysfunction in HepG2 cells by palmitic acid. *Nutrients*, 11(9), p.1979.
- Arroyo, J.D., Chevillet, J.R., Kroh, E.M., Ruf, I.K., Pritchard, C.C., Gibson, D.F., Mitchell, P.S., Bennett, C.F., Pogosova-Agadjanian, E.L., Stirewalt, D.L. and Tait, J.F., 2011. Argonaute2 complexes carry a population of circulating microRNAs independent of vesicles in human plasma. *Proceedings of the National Academy of Sciences*, 108(12), pp.5003-5008.
- Ashton, L., 2021. CBD and Liver Damage: How Does It Affect Liver Functions?
- Atalay, S., Jarocka-Karpowicz, I. and Skrzydlewska, E., 2019. Antioxidative and anti-inflammatory properties of cannabidiol. *Antioxidants*, 9(1), p.21.

- Ayakannu, R., Abdullah, N.A., Radhakrishnan, A.K., Raj, V.L. and Liam, C.K., 2019. Relationship between various cytokines implicated in asthma. *Human immunology*, 80(9), pp.755-763.
- Bae, T., Hallis, S.P. and Kwak, M.K., 2024. Hypoxia, oxidative stress, and the interplay of HIFs and NRF2 signalling in cancer. *Experimental & Molecular Medicine*, 56(3), pp.501-514.
- Baldassarre, M., Giannone, F.A., Napoli, L., Tovoli, A., Ricci, C.S., Tufoni, M. and Caraceni, P., 2013. The endocannabinoid system in advanced liver cirrhosis: pathophysiological implication and future perspectives. *Liver International*, 33(9), pp.1298-1308.
- Bazwinsky-Wutschke, I., Zipprich, A. and Dehghani, F., 2019. Endocannabinoid system in hepatic glucose metabolism, fatty liver disease, and cirrhosis. *International Journal of Molecular Sciences*, 20(10), p.2516.
- BD Editors., 2017, Apoptosis., 06-06-2017: www.biologydictionary.net/apoptosis
- Bickel, M., 1993. The role of interleukin-8 in inflammation and mechanisms of regulation. *Journal of periodontology*, 64(5 Supply), pp.456-460.
- Booz, G.W., 2011. Cannabidiol as an emergent therapeutic strategy for lessening the impact of inflammation on oxidative stress. *Free Radical Biology and Medicine*, 51(5), pp.1054-1061.
- Brewer, S., 2020. CBD: The Essential Guide to Health and Wellness. Simon and Schuster.
- Burstein, S., 2015. Cannabidiol (CBD) and its analogs: a review of their effects on inflammation. *Bioorganic & medicinal chemistry*, 23(7), pp.1377-1385.
- Chakraborty, C., Doss, C.G.P., Bandyopadhyay, S. and Agoramoorthy, G., 2014. Influence of miRNA in insulin signalling pathway and insulin resistance: micro-molecules with a major role in type-2 diabetes. *Wiley interdisciplinary reviews: RNA*, 5(5), pp.697-712.
- Chen, L., Deng, H., Cui, H., Fang, J., Zuo, Z., Deng, J., Li, Y., Wang, X. and Zhao, L., 2018. Inflammatory responses and inflammation-associated diseases in organs. *Oncotarget*, 9(6), p.7204.
- Cho, N., Shaw, J.E., Karuranga, S., Huang, Y., da Rocha Fernandes, J.D., Ohlrogge, A.W. and Malanda, B., 2018. IDF Diabetes Atlas: Global estimates of diabetes prevalence for 2017 and projections for 2045. *Diabetes research and clinical practice*, 138, pp.271-281.
- Chua, J.T., Argueta, D.A., DiPatrizio, N.V., Kovesdy, C.P., Vaziri, N.D., Kalantar-Zadeh, K. and Moradi, H., 2019. Endocannabinoid system and the kidneys: from renal physiology to injury and disease. *Cannabis and cannabinoid research*, 4(1), pp.10-20.
- Campos, A.C., Fogaça, M.V., Scarante, F.F., Joca, S.R., Sales, A.J., Gomes, F.V., Sonogo, A.B., Rodrigues, N.S., Galve-Roperh, I. and Guimarães, F.S., 2017. Plastic and neuroprotective mechanisms involved in the therapeutic effects of cannabidiol in psychiatric disorders. *Frontiers in pharmacology*, 8, p.269.
- Coope, A., Torsoni, A.S. and Velloso, L.A., 2016. Mechanisms in endocrinology: metabolic and inflammatory pathways on the pathogenesis of type 2 diabetes. *European journal of*

endocrinology, 174(5), pp. R175-R187.

Danielsson, A.K., Lundin, A., Yaregal, A., Östenson, C.G., Allebeck, P. and Agardh, E.E., 2016. Cannabis use as risk or protection for type 2 diabetes: a longitudinal study of 18 000 Swedish men and women. *Journal of diabetes research*, 2016.

Di Marzo, V., 2008. The endocannabinoid system in obesity and type 2 diabetes. *Diabetology*, 51(8), pp.1356-1367.

Eizirik, D.L., Pasquali, L. and Cnop, M., 2020. Pancreatic β -cells in type 1 and type 2 diabetes mellitus: different pathways to failure. *Nature Reviews Endocrinology*, 16(7), pp.349-362.

Ekiner, S.A., Gęgotek, A. and Skrzydlewska, E., 2022. The molecular activity of cannabidiol in the regulation of Nrf2 system interacting with NF- κ B pathway under oxidative stress. *Redox Biology*, p.102489.

Elmore, S., 2007. Apoptosis: a review of programmed cell death. *Toxicologic pathology*, 35(4), pp.495-516.

Fachette, L., 2018, Diabetes and Marijuana: A Possible Treatment? 29-10-2020: www.thediabetescouncil.com/diabetes-and-marijuana

Farhat, T., Simons-Morton, B. and Luk, J.W., 2011. Psychosocial correlates of adolescent marijuana use: Variations by status of marijuana use. *Addictive Behaviours*, 36(4), pp.404-407.

Farokhnia, M., McDiarmid, G.R., Newmeyer, M.N., Munjal, V., Abulseoud, O.A., Huestis, M.A. and Leggio, L., 2020. Effects of oral, smoked, and vaporized cannabis on endocrine pathways related to appetite and metabolism: a randomized, double-blind, placebo-controlled, human laboratory study. *Translational psychiatry*, 10(1), pp.1-11.

Feng, J., Xing, W. and Xie, L., 2016. Regulatory roles of microRNAs in diabetes. *International journal of molecular sciences*, 17(10), p.1729.

Fletcher, B., Gulanick, M. and Lamendola, C., 2002. Risk factors for type 2 diabetes mellitus. *Journal of Cardiovascular Nursing*, 16(2), pp.17-23.

Foley, N.H. and O'Neill, L.A., 2012. miR-107: a Toll-like receptor-regulated miRNA dysregulated in obesity and type II diabetes. *Journal of leukocyte biology*, 92(3), pp.521-527.

García-Arencibia, M., González, S., de Lago, E., Ramos, J.A., Mechoulam, R. and Fernández-Ruiz, J., 2007. Evaluation of the neuroprotective effect of cannabinoids in a rat model of Parkinson's disease: importance of antioxidant and cannabinoid receptor-independent properties. *Brain research*, 1134, pp.162-170.

García-Pastor, C., Benito-Martínez, S., Moreno-Manzano, V., Fernández-Martínez, A.B. and Lucio-Cazaña, F.J., 2019. Mechanism and consequences of the impaired Hif-1 α response to hypoxia in human proximal tubular HK-2 cells exposed to high glucose. *Scientific reports*, 9(1), p.15868.

- Goldstein, B.J., 2002. Insulin resistance as the core defect in type 2 diabetes mellitus. *The American journal of cardiology*, 90(5), pp.3-10.
- Gonçalves, J., Rosado, T., Soares, S., Simão, A.Y., Caramelo, D., Luís, Â., Fernández, N., Barroso, M., Gallardo, E. and Duarte, A.P., 2019. Cannabis and its secondary metabolites: Their use as therapeutic drugs, toxicological aspects, and analytical determination. *Medicines*, 6(1), p.31.
- Goswami, R. and Kaplan, M.H., 2011. A brief history of IL-9. *The Journal of Immunology*, 186(6), pp.3283-3288.
- Gregory, R.I., Yan, K.P., Amuthan, G., 2004. The microprocessor complex mediates the genesis of microRNAs. *Nature*, 432: 235 – 240.
- Griffith-Jones, S., Grocock, R.J., van Dongen, S., Bateman, A., Enright, A.J., 2006. miRBase: microRNA sequences, targets and gene nomenclature. *Nucleic Acids Research*, 34: D140 –144, Doi: 10.1093/nar/gkj112.
- Grotenhermen, F. and Müller-Vahl, K., 2016. Medicinal uses of marijuana and cannabinoids. *Critical Reviews in Plant Sciences*, 35(5-6), pp.378-405.
- Gruden, G., Barutta, F., Kunos, G. and Pacher, P., 2016. Role of the endocannabinoid system in diabetes and diabetic complications. *British journal of pharmacology*, 173(7), pp.1116-1127.
- Gunton, J.E., 2020. Hypoxia-inducible factors and diabetes. *The Journal of clinical investigation*, 130(10), pp.5063-5073.
- Guttler, T., & Gorlich, D., 2011. Ran-dependant nuclear export mediators: a structural perspective. *European Molecular Biology Organization Journal*, 30: 3457 – 3474.
- Hameed, I., Masoodi, S.R., Mir, S.A., Nabi, M., Ghazanfar, K. and Ganai, B.A., 2015. Type 2 diabetes mellitus: from a metabolic disorder to an inflammatory condition. *World journal of diabetes*, 6(4), p.598.
- Han, H.S., Kang, G., Kim, J.S., Choi, B.H. and Koo, S.H., 2016. Regulation of glucose metabolism from a liver-centric perspective. *Experimental & molecular medicine*, 48(3), pp. e218-e218.
- Hoffman, M., 2023, Diabetes and Inflammation
- Hongmei, Z., 2012. Extrinsic and intrinsic apoptosis signal pathway review. In *Apoptosis and medicine*. Intech Open.
- Horváth, B., Mukhopadhyay, P., Haskó, G. and Pacher, P., 2012. The endocannabinoid system and plant-derived cannabinoids in diabetes and diabetic complications. *The American journal of pathology*, 180(2), pp.432-442.
- Hryciw, D.H. and McAinch, A.J., 2016. Cannabinoid receptors in the kidney. *Current opinion in nephrology and hypertension*, 25(5), pp.459-464.

Hu, Y., Chen, Y., Ding, L., He, X., Takahashi, Y., Gao, Y., Shen, W., Cheng, R., Chen, Q., Qi, X. and Boulton, M.E., 2013. Pathogenic role of diabetes-induced PPAR- α down-regulation in microvascular dysfunction. *Proceedings of the National Academy of Sciences*, 110(38), pp.15401-15406.

Ighodaro, O.M. and Akinloye, O.A., 2018. First line defence antioxidants-superoxide dismutase (SOD), catalase (CAT) and glutathione peroxidase (GPX): Their fundamental role in the entire antioxidant defence grid. *Alexandria journal of medicine*, 54(4), pp.287-293.

Jedrzejczak-Silicka, M., 2017. History of cell culture. *New insights into cell culture technology*, 1, p.13.

Jordan, S.D., Krüger, M., Willmes, D.M., Redemann, N., Wunderlich, F.T., Brönneke, H.S., Merkwirth, C., Kashkar, H., Olkkonen, V.M., Böttger, T. and Braun, T., 2011. Obesity-induced overexpression of miRNA-143 inhibits insulin-stimulated AKT activation and impairs glucose metabolism. *Nature cell biology*, 13(4), pp.434-446.

Jîtcă, G., Ősz, B.E., Vari, C.E., Rusz, C.M., Tero-Vescan, A. and Puşcaş, A., 2023. Cannabidiol: Bridge between Antioxidant Effect, Cellular Protection, and Cognitive and Physical Performance. *Antioxidants*, 12(2), p.485.

Jo, M.J., Kim, B.G., Kim, W.Y., Lee, D.H., Yun, H.K., Jeong, S., Park, S.H., Kim, B.R., Kim, J.L., Kim, D.Y. and Lee, S.I., 2021. Cannabidiol suppresses angiogenesis and stemness of breast cancer cells by downregulation of hypoxia-inducible factors-1 α . *Cancers*, 13(22), p.5667.

Juknat, A., Gao, F., Coppola, G., Vogel, Z. and Kozela, E., 2019. miRNA expression profiles and molecular networks in resting and LPS-activated BV-2 microglia—Effect of cannabinoids. *PloS one*, 14(2), p.e0212039.

Khaksar, S., Bigdeli, M., Samiee, A. and Shirazi-Zand, Z., 2022. Antioxidant and anti-apoptotic effects of cannabidiol in model of ischemic stroke in rats. *Brain Research Bulletin*, 180, pp.118-130.

Khosropoor, S., Alavi, M.S., Etemad, L. and Roohbakhsh, A., 2023. Cannabidiol goes nuclear: The role of PPAR γ . *Phytomedicine*, p.154771.

Krol, J., Loedige, I. and Filipowicz, W., 2010. The widespread regulation of microRNA biogenesis, function and decay. *Nature Reviews Genetics*, 11(9), pp.597-610.

Krzystek-Korpacka, M., Neubauer, K. and Matusiewicz, M., 2009. Platelet-derived growth factor-BB reflects clinical, inflammatory and angiogenic disease activity and oxidative stress in inflammatory bowel disease. *Clinical biochemistry*, 42(16-17), pp.1602-1609.

Kowalczyk, A., Marycz, K., Kornicka-Garbowska, K., Kornicka, J., Bujalska-Zadrożny, M. and Groborz, S., 2022. Cannabidiol (CBD) protects adipose-derived mesenchymal stem cells (ASCs) against endoplasmic reticulum stress development and its complications. *International Journal of Environmental Research and Public Health*, 19(17), p.10864.

Kuhn, D.E., Martin, M.M., Feldman, D.S., Terry, A.V., Nuovo, G.J. and Elton, T.S., 2008.

Experimental validation of miRNA targets. *Methods*, 44(1): 47 – 54.

Kumar, A. and Ameeramja, J., 2021. Cell viability and apoptotic assays to assess drug efficacy. In *Protocol Handbook for Cancer Biology* (pp. 7-22). Academic Press.

Indira, M. and Abhilash, P.A., 2013. Role of NF-Kappa B (NF-κB) in diabetes. *Onco Therapeutics*, 4(2).

La Sala, L., Mrakic-Sposta, S., Tagliabue, E., Prattichizzo, F., Micheloni, S., Sangalli, E., Specchia, C., Uccellatore, A.C., Lupini, S., Spinetti, G. and De Candia, P., 2019. Circulating microRNA-21 is an early predictor of ROS-mediated damage in subjects with high risk of developing diabetes and in drug-naïve T2D. *Cardiovascular diabetology*, 18(1), pp.1-12.

Lee, Y., Joen, K., Lee, J.T., 2002. MicroRNA maturation: stepwise processing and subcellular localization. *European Molecular Biology Organization Journal*, 21: 4663 –4670.

Li, H.S., Zhou, Y.N., Li, L., Li, S.F., Long, D., Chen, X.L., Zhang, J.B., Feng, L. and Li, Y.P., 2019. HIF-1α protects against oxidative stress by directly targeting mitochondria. *Redox biology*, 25, p.101109.

Li, Y.F., Jing, Y., Hao, J., Frankfort, N.C., Zhou, X., Shen, B., Liu, X., Wang, L. and Li, R., 2013. MicroRNA-21 in the pathogenesis of acute kidney injury. *Protein & cell*, 4(11), pp.813-819.

Lingappan, K., 2018. NF-κB in oxidative stress. *Current opinion in toxicology*, 7, pp.81-86.

Lisano, J., 2020. CBD and Exercise Related Inflammation: Is there something there?

Liu, R., Bian, Y., Liu, L., Liu, L., Liu, X. and Ma, S., 2022. Molecular pathways associated with oxidative stress and their potential applications in radiotherapy. *International Journal of Molecular Medicine*, 49(5), pp.1-11.

Livak, K.J. and Schmittgen, T.D., 2001. Analysis of relative gene expression data using real-time quantitative PCR and the 2⁻ΔΔCT method. *methods*, 25(4), pp.402-408.

Loftis, A.D. and Reeves, W.K., 2012. Principles of real-time PCR. *Veterinary PCR diagnostics*, 3.

Lu, H.C. and Mackie, K., 2021. Review of the endocannabinoid system. *Biological Psychiatry: Cognitive Neuroscience and Neuroimaging*, 6(6), pp.607-615.

Lubaale, E.C. and Mavundla, S.D., 2019. Decriminalisation of cannabis for personal use in South Africa. *African Human Rights Law Journal*, 19(2), pp.819-842.

Lubos, E., Loscalzo, J. and Handy, D.E., 2011. Glutathione peroxidase-1 in health and disease: from molecular mechanisms to therapeutic opportunities.

Luo, M., Xu, C., Luo, Y., Wang, G., Wu, J. and Wan, Q., 2020. Circulating miR-103 family as potential biomarkers for type 2 diabetes through targeting CAV-1 and SFRP4. *Acta*

diabetologist, 57(3), pp.309-322.

Ma, Q., 2013. Role of nrf2 in oxidative stress and toxicity. *Annual review of pharmacology and toxicology*, 53(1), pp.401-426.

Margis, R., Dunand, C., Teixeira, F.K. and Margis-Pinheiro, M., 2008. Glutathione peroxidase family—an evolutionary overview. *The FEBS journal*, 275(15), pp.3959-3970.

Marasco, M.R., Conteh, A.M., Reissaus, C.A., Cupit, J.E., Appleman, E.M., Mirmira, R.G. and Linnemann, A.K., 2018. Interleukin-6 reduces β -cell oxidative stress by linking autophagy with the antioxidant response. *Diabetes*, 67(8), pp.1576-1588.

Maritim, A.C., Sanders, A. and Watkins lii, J.B., 2003. Diabetes, oxidative stress, and antioxidants: a review. *Journal of biochemical and molecular toxicology*, 17(1), pp.24-38.

Martin A, Lee., 2011. How CBD works. Available at: www.projectcbd.org/science/how-cbd-works (Accessed: 11 August, 2011)

Mattes, R.G., Espinosa, M.L., Oh, S.S., Anatrella, E.M. and Urteaga, E.M., 2020. Cannabidiol (CBD) Use in Type 2 Diabetes: A Case Report. *Diabetes Spectrum*.

Maule, W.J., 2015. Medical uses of marijuana (*Cannabis sativa*): fact or fallacy? *British journal of biomedical science*, 72(2), pp.85-91.

McPartland, J.M., Duncan, M., Di Marzo, V. and Pertwee, R.G., 2015. Are cannabidiol and Δ^9 -tetrahydrocannabivarin negative modulators of the endocannabinoid system? A systematic review. *British journal of pharmacology*, 172(3), pp.737-753.

Mechoulam, R. and Hanuš, L., 2002. Cannabidiol: an overview of some chemical and pharmacological aspects. Part I: chemical aspects. *Chemistry and physics of lipids*, 121(1-2), pp.35-43.

Méndez, I., Vázquez-Cuevas, F., Hernández-Muñoz, R., Valente-Godínez, H., Vázquez-Martínez, O. and Díaz-Muñoz, M., 2017. Redox Reactions in the Physiopathology of the Liver. *Redox-Principles and Advanced Applications*.

Mihaylova, Z., Tsikandelova, R., Sanimirov, P., Gateva, N., Mitev, V. and Ishkitiev, N., 2018. Role of PDGF-BB in proliferation, differentiation and maintaining stem cell properties of PDL cells in vitro. *Archives of oral biology*, 85, pp.1-9.

Mihir, N., Nakrani., Robert, H., Anjum, F., 2020, Physiology, Glucose Metabolism., 14-08-2020: www.ncbi.nlm.nih.gov/books/NBK300599

Mone, P., de Donato, A., Varzideh, F., Kansakar, U., Jankauskas, S.S., Pansini, A. and Santulli, G., 2022. Functional role of miR-34a in diabetes and frailty. *Frontiers in Aging*, 3, p.949924.

Muralidhar Reddy, P., Maurya, N. and Velmurugan, B.K., 2019. Medicinal use of synthetic cannabinoids—a mini review. *Current pharmacology reports*, 5, pp.1-13.

Muzio, G., Barrera, G. and Pizzimenti, S., 2021. Peroxisome proliferator-activated receptors (PPARs) and oxidative stress in physiological conditions and in cancer. *Antioxidants*, 10(11), p.1734.

Newman, T., 2018, The liver: Structure, function and disease., 02-03-2018:
www.medicalnewstoday.com>articles

Nandi, A., Yan, L.J., Jana, C.K. and Das, N., 2019. Role of catalase in oxidative stress-and age-associated degenerative diseases. *Oxidative medicine and cellular longevity*, 2019.

Ngo, V. and Duennwald, M.L., 2022. Nrf2 and Oxidative Stress: A General Overview of Mechanisms and Implications in Human Disease. *Antioxidants*, 11(12), p.2345.

Nguyen, T., Thomas, B.F. and Zhang, Y., 2019. Overcoming the psychiatric side effects of the cannabinoid CB1 receptor antagonists: current approaches for therapeutics development. *Current topics in medicinal chemistry*, 19(16), pp.1418-1435.

Oguntibeju, O.O., 2019. Type 2 diabetes mellitus, oxidative stress and inflammation: examining the links. *International journal of physiology, pathophysiology and pharmacology*, 11(3), p.45.

Ozougwu, J.C., Obimba, K.C., Belonwu, C.D. and Unakalamba, C.B., 2013. The pathogenesis and pathophysiology of type 1 and type 2 diabetes mellitus. *Journal of physiology and pathophysiology*, 4(4), pp.46-57.

Ozsolak, F. and Milos, P.M., 2011. Single-molecule direct RNA sequencing without cDNA synthesis. *Wiley Interdisciplinary Reviews: RNA*, 2(4), pp.565-570.

Pagano, S., Coniglio, M., Valenti, C., Federici, M.I., Lombardo, G., Cianetti, S. and Marinucci, L., 2020. Biological effects of Cannabidiol on normal human healthy cell populations: Systematic review of the literature. *Biomedicine & Pharmacotherapy*, 132, p.110728.

Patel, S. and Santani, D., 2009. Role of NF- κ B in the pathogenesis of diabetes and its associated complications. *Pharmacological reports*, 61(4), pp.595-603.

Panahi, G., Pasalar, P., Zare, M., Rizzuto, R. and Meshkani, R., 2018. High glucose induces inflammatory responses in HepG2 cells via the oxidative stress-mediated activation of NF- κ B, and MAPK pathways in HepG2 cells. *Archives of physiology and biochemistry*, 124(5), pp.468-474.

Penner, E.A., Buettner, H. and Mittleman, M.A., 2013. The impact of marijuana uses on glucose, insulin, and insulin resistance among US adults. *The American journal of medicine*, 126(7), pp.583-589.

Petrocellis, L.D., Cascio, M.G. and Marzo, V.D., 2004. The endocannabinoid system: a general view and latest additions. *British journal of pharmacology*, 141(5), pp.765-774.

Qu, D., Liu, J., Lau, C.W. and Huang, Y., 2014. IL-6 in diabetes and cardiovascular complications. *British journal of pharmacology*, 171(15), pp.3595-3603.

- Rains, J.L. and Jain, S.K., 2011. Oxidative stress, insulin signalling, and diabetes. *Free Radical Biology and Medicine*, 50(5), pp.567-575.
- Reinhart, B.J., Slack, F.J. Basson, M., 2000. The 21-nucleotide let-7 RNA regulates developmental timing in *Caenorhabditis elegans*. *Nature*, 403: 901 – 906.
- Rodríguez de Fonseca, F., Del Arco, I., Bermudez-Silva, F.J., Bilbao, A., Cippitelli, A. and Navarro, M., 2005. The endocannabinoid system: physiology and pharmacology. *Alcohol and Alcoholism*, 40(1), pp.2-14.
- Roland, J., 2014, SignsofInsulinResistance.,02-09-2014:
www.healthline.com>health>diabetes>insuline-resisatnce
- Rong, Y., Bao, W., Shan, Z., Liu, J., Yu, X., Xia, S., Gao, H., Wang, X., Yao, P., Hu, F.B. and Liu, L., 2013. Increased microRNA-146a levels in plasma of patients with newly diagnosed type 2 diabetes mellitus. *PloS one*, 8(9), p.e73272.
- Rui, L., 2011. Energy metabolism in the liver. *Comprehensive physiology*, 4(1), pp.177-197.
- Rose-John, S., 2018. Interleukin-6 family cytokines. *Cold Spring Harbour perspectives in biology*, 10(2), p.a028415.
- Sabat, R., Grütz, G., Warszawska, K., Kirsch, S., Witte, E., Wolk, K. and Geginat, J., 2010. Biology of interleukin-10. *Cytokine & growth factor reviews*, 21(5), pp.331-344.
- Sand, M., 2014. The pathway of miRNA maturation. In Arenz, C (ed). *MiRNA Maturation: Methods & Protocols, Methods in Molecular Biology*. Springer Science & Business Media New York, 1095: 1 – 10.
- Sand, M., Skrygan, M., Georgas, D., 2011. Expression levels of the microRNA maturing microprocessor complex component DGCR8 and the RNA-induced silencing complex (RISC) components Argonaute-1, Argonaute-2, PACT, TARBP1 and TARBP2 in epithelial skin cancer. *Molecular Carcinogenesis*, 51: 916 – 922.
- Segeritz, C.P. and Vallier, L., 2017. Cell culture: Growing cells as model systems in vitro. In *Basic science methods for clinical researchers* (pp. 151-172). Academic Press.
- Sekar, D., Venugopal, B., Sekar, P. and Ramalingam, K., 2016. Role of microRNA 21 in diabetes and associated/related diseases. *Gene*, 582(1), pp.14-18.
- Serasanambati, M. and Chilakapati, S.R., 2016. Function of nuclear factor kappa B (NF-κB) in human diseases-a review. *South Indian Journal of Biological Sciences*, 2(4), pp.368-87.
- Sharif, S., Van der Graaf, Y., Cramer, M.J., Kapelle, L.J., de Borst, G.J., Visseren, F.L., Westerink, J. and SMART study group R. van Petersen BGF Dinther A. Algra Y. van der Graaf DE Grobbee GEHM Rutten FLJ Visseren GJ de Borst LJ Kappelle T. Leiner HM

- Nathoe., 2021. Low-grade inflammation as a risk factor for cardiovascular events and all-cause mortality in patients with type 2 diabetes. *Cardiovascular Diabetology*, 20, pp.1-8.
- Staeher, P., Hother-Nielsen, O. and Beck-Nielsen, H., 2004. The role of the liver in type 2 diabetes. *Reviews in endocrine & metabolic disorders*, 5(2), p.105.
- Stanley, C.P., Hind, W.H. and O'Sullivan, S.E., 2013. Is the cardiovascular system a therapeutic target for cannabidiol? *British journal of clinical pharmacology*, 75(2), pp.313-322.
- Stinkens, R., Goossens, G.H., Jocken, J.W. and Blaak, E.E., 2015. Targeting fatty acid metabolism to improve glucose metabolism. *Obesity Reviews*, 16(9), pp.715-757.
- Stroppler, M.C., 2020, Insulin Resistance., 24-02-2021: www.medicinenet.com>Insulin_resistance>article
- Su, W., Cao, R., Zhang, X.Y. and Guan, Y., 2020. Aquaporins in the kidney: physiology and pathophysiology. *American Journal of Physiology-Renal Physiology*, 318(1), pp. F193-F203.
- Subramaniyan, D., & Kumar, A., 2017. *Citral Protects High Glucose Induced Oxidative Damage Journal of Clinical and Diagnostic Research* (Vol. 11, Issue 8). www.jcdr.net
- Svíženská, I., Dubový, P. and Šulcová, A., 2008. Cannabinoid receptors 1 and 2 (CB1 and CB2), their distribution, ligands and functional involvement in nervous system structures—a short review. *Pharmacology Biochemistry and Behaviour*, 90(4), pp.501-511.
- Tang, J., Yao, D., Yan, H., Chen, X., Wang, L. and Zhan, H., 2019. The role of MicroRNAs in the pathogenesis of diabetic nephropathy. *International journal of endocrinology*, 2019.
- Taylor, R., 2012. Insulin resistance and type 2 diabetes. *Diabetes*, 61(4), pp.778-779.
- Tehrani, H.S. and Moosavi-Movahedi, A.A., 2018. Catalase and its mysteries. *Progress in biophysics and molecular biology*, 140, pp.5-12.
- Tiwari, B.K., Pandey, K.B., Abidi, A.B. and Rizvi, S.I., 2013. Markers of oxidative stress during diabetes mellitus. *Journal of biomarkers*, 2013.
- Trefts E, Gannon M, Wasserman DH. The liver. *Curr Biol.*, 2017 Nov 6;27(21): R1147-R1151. Doi: 10.1016/j.cub.2017.09.019. PMID: 29112863; PMCID: PMC5897118.
- Tsalamandris, S., Antonopoulos, A.S., Oikonomou, E., Papamikroulis, G.A., Vogiatzi, G., Papaioannou, S., Deftereos, S. and Tousoulis, D., 2019. The role of inflammation in diabetes: current concepts and future perspectives. *European cardiology review*, 14(1), p.50.
- Van Rensburg, R., Pillay-Fuentes Lorente, V., Blockman, M., Moodley, K., Wilmshurst, J.M. and Decloedt, E.H., 2020. Medical cannabis: What practitioners need to know. *South African Medical Journal*, 110(3), pp.192-196.
- Vilotić, A., Nacka-Aleksić, M., Pirković, A., Bojić-Trbojević, Ž., Dekanski, D. and Jovanović Krivokuća, M., 2022. IL-6 and IL-8: an overview of their roles in healthy and pathological pregnancies. *International journal of molecular sciences*, 23(23), p.14574.

Wang, J., & Guo, H., 2019. Astragal side IV ameliorates high glucose-induced HK-2 cell apoptosis and oxidative stress by regulating the Nrf2/ARE signalling pathway. *Experimental and Therapeutic Medicine*. <https://doi.org/10.3892/etm.2019.7495>

Wang, H.W., Noland, C., Siridechadilok, B., 2009. Structural insights into RNA processing by the human RISC-loading complex. *Nature Structural & Molecular Biology*, 16 :1148 – 1153

Wang, W.X., Wilfred, B.R., Baldwin, D.A., Isett, R.B., Ren, N., Stromberg, A. and Nelson, P.T., 2008. Focus on RNA isolation: obtaining RNA for microRNA (miRNA) expression profiling analyses of neural tissue. *Biochimica et Biophysica Acta (BBA)-Gene Regulatory Mechanisms*, 1779(11), pp.749-757.

Way, J.M., Harrington, W.W., Brown, K.K., Gottschalk, W.K., Sundseth, S.S., Mansfield, T.A., Ramachandran, R.K., Willson, T.M. and Klierer, S.A., 2001. Comprehensive messenger ribonucleic acid profiling reveals that peroxisome proliferator-activated receptor γ activation has coordinate effects on gene expression in multiple insulin-sensitive tissues. *Endocrinology*, 142(3), pp.1269-1277.

Wegner, M., Winiarska, H., Bobkiewicz-Kozłowska, T. and Dworacka, M., 2008. IL-12 serum levels in patients with type 2 diabetes treated with sulphonylureas. *Cytokine*, 42(3), pp.312-316.

Weiss, L., Zeira, M., Reich, S., Slavin, S., Raz, I., Mechoulam, R. and Gallily, R., 2008. Cannabidiol arrests onset of autoimmune diabetes in NOD mice. *Neuropharmacology*, 54(1), pp.244-249.

Xiao, H., Gu, Z., Wang, G. and Zhao, T., 2013. The possible mechanisms underlying the impairment of HIF-1 α pathway signalling in hyperglycaemia and the beneficial effects of certain therapies. *International journal of medical sciences*, 10(10), p.1412.

Xu, Q., He, C., Xiao, C. and Chen, X., 2016. Reactive oxygen species (ROS) responsive polymers for biomedical applications. *Macromolecular bioscience*, 16(5), pp.635-646.

Yaghini, N., Mahmoodi, M., Asadikaram, G., Hassanshahi, G., Khoramdelazed, H. and Arababadi, M.K., 2011. Serum levels of interleukin 10 (IL-10) in patients with type 2 diabetes. *Iranian Red Crescent Medical Journal*, 13(10), pp.752-753.

Ying, S.Y., Chang, D.C. and Lin, S.L., 2008. The microRNA (miRNA): overview of the RNA genes that modulate gene function. *Molecular biotechnology*, 38, pp.257-268.

Ziello, J.E., Jovin, I.S. and Huang, Y., 2007. Hypoxia-Inducible Factor (HIF)-1 regulatory pathway and its potential for therapeutic intervention in malignancy and ischemia. *The Yale journal of biology and medicine*, 80(2), p.51.

Zundler, S. and Neurath, M.F., 2015. Interleukin-12: Functional activities and implications for disease. *Cytokine & growth factor reviews*, 26(5), pp.559-568.

APPENDIX A

All the Nanodrop Results

Table 1. Table showing the nanodrop results for RNA isolated after 48 hours, used for miRNA analysis

Sample	Concentration (ng/ µl)	A260/280	A260/230
Control	517,4	2,11	1,93
Glucose	471,7	2,06	1,57
Low CBD	368,8	2,07	2,02
High CBD	160,7	2,02	1,88
Low CBD & Glucose	495,8	2,06	2,00
High CBD& Glucose	578,6	2,10	2,15

Table 2. Table showing the nanodrop results for RNA isolated after 72 hours, used for miRNA analysis

Samples	Concentration (ng/ µl)	A260/280	A260/230
Control	516,5	2,09	1,78
Glucose	452,9	2,07	2,03
Low CBD	217,3	2,03	2,07
High CBD	285,3	2,04	1,94
Low CBD & Glucose	683,7	2,08	2,13
High CBD& Glucose	350,8	2,06	1,85

Table 3. Table showing the nanodrop results for RNA isolated after 48 hours, used for mRNA analysis

Samples	Concentration (ng/ µl)	A260/280	A260/230
Control	5434,1	2,11	1,56

Glucose	8064	2,04	1,66
Low CBD	4977,8	2,10	1,86
High CBD	6899	2,08	1,98
Low CBD & Glucose	7201,3	2,07	2,07
High CBD& Glucose	9194,3	2,07	1,92

Table 4. Table showing the nanodrop results for RNA isolated after 72 hours, used for mRNA analysis

Samples	Concentration (ng/ µl)	A260/280	A260/230
Control	4747,5	2,12	1,68
Glucose	4734	2,07	1,44
Low CBD	4906,9	2,10	1,92
High CBD	4996,7	2,12	2,02
Low CBD & Glucose	3566,3	2,08	1,53
High CBD& Glucose	4040,9	2,09	1,68

HEALTH AND WELLNESS SCIENCES RESEARCH ETHICS COMMITTEE (CPUT HWS-REC)
Registration Number NHREC: REC- 230408-014

P.O. Box 1906 • Bellville 7535 South Africa
Symphony Road Bellville 7535
Tel: +27 21 959 6917
Email: sethn@cput.ac.za

16 February 2024
REC Approval Reference No:
CPUT/HWS-REC 2021/H24 (Renewal)

Faculty of Health and Wellness Sciences

Dear Ms Chanelle Rinkwest - 212270346

Re: APPLICATION TO THE CPUT/HWS-REC FOR ETHICS CLEARANCE

Approval was granted by the Health and Wellness Sciences-REC to **Ms. C Rinkwest** for ethical clearance. This approval is for research activities related to research for **Ms. C Rinkwest** at Cape Peninsula University of Technology.

TITLE: The in vitro effects of Cannabinol on high glucose levels with miRNA profiling

Supervisors: Prof. T Matsha-Erasmus and Dr. S Raghubeer

Comment:

Approval will not extend beyond 17 February 2025. An extension should be applied for 6 weeks before this expiry date should data collection and use/analysis of data, information and/or samples for this study continue beyond this date.

The investigator(s) should understand the ethical conditions under which they are authorized to carry out this study and they should be compliant to these conditions. It is required that the investigator(s) complete an **annual progress report** that should be submitted to the CPUT HWS-REC in December of that particular year, for the CPUT HWS-REC to be kept informed of the progress and of any problems you may have encountered.

Kind Regards



Dr. Samantha Meyer
Deputy Chairperson – Research Ethics Committee
Faculty of Health and Wellness Sciences